Changes in Brain Functional Activation during Resting and Locomotor States after Unilateral Nigrostriatal Damage in Rats

J. Yang[a,f], **T.R. Sadler**[d], **T.K. Givrad**[e], **J.-M.I. Maarek**[e], and **D.P. Holschneider**[a,b,c,f,*]

a*Department of Psychiatry and the Behavioral Sciences, University of Southern California, Keck School of Medicine, Los Angeles, CA 90089-9121, USA*

b*Department of Neurology, University of Southern California, Keck School of Medicine, Los Angeles, CA 90033, USA*

c*Department of Cell and Neurobiology, University of Southern California, Keck School of Medicine, Los Angeles, CA 90033, USA*

d*Department of Pathology, University of Southern California, Keck School of Medicine, Los Angeles, CA 90033, USA*

e*Department of Biomedical Engineering, University of Southern, California School of Engineering, Los Angeles, CA, USA*

f*Greater Los Angeles VA Healthcare System, Los Angeles, CA 90073, USA*

Abstract

To evaluate functional neuronal compensation after partial damage to the nigrostriatal system, we lesioned rats unilaterally in the striatum with 6-hydroxydopamine. Five weeks later, cerebral perfusion was mapped at rest or during treadmill walking using [^{14}C]-iodoantipyrine. Regional CBF-related tissue radioactivity (CBF-TR) was quantified by autoradiography and analyzed by statistical parametric mapping and region-of-interest analysis. Lesions were confirmed by tyrosine hydroxylase immunohistochemistry and changes in rotational locomotor activity.

Functional compensations were bilateral and differed at rest and during treadmill walking. Consistent with the classic view of striatopallidal connections, CBF-TR of lesioned compared to sham-lesioned rats increased in the ipsilateral subthalamic nucleus (STN) and internal globus pallidus, and decreased in the striatum and external globus pallidus. Contrary to the classic view, CBF-TR increased in the ipsilateral ventral lateral, ventral anterior thalamus and motor cortex, as well as in the central medial thalamus, midline cerebellum, and contralateral STN.

During walking, perfusion decreased in lesioned compared to sham-lesioned rats across the ipsilateral striato-pallidal-thalamic-cortical motor circuit. Compensatory increases were seen bilaterally in the ventromedial thalamus and red nucleus, in the contralateral STN, anterior substantia nigra, subiculum, motor cortex, and in midline cerebellum. Enhanced recruitment of associative sensory areas was noted cortically and subcortically.

Future models of compensatory changes after nigrostriatal damage need to address the effects of increased neural activity by residual dopaminergic neurons, interhemispheric interactions and differences between resting and locomotor states. Identification of sites at which functional

---

*Corresponding author. University of Southern California, Keck School of Medicine, Department of Cell and Neurobiology, 1333 San Pablo St., BMT 403, MC 9112, Los Angeles, CA 90089-9112, USA. Fax: +1 323 442 1587. *E-mail address*: holschne@usc.edu (D.P. Holschneider).

Uncited reference
Alexander and Crutcher, 1990

compensation occurs may define useful future targets for neurorehabilitative or neurorestorative interventions in Parkinson's disease.

Keywords

Brain mapping; Functional neuroimaging; Cerebral blood flow; Plasticity; Hemiparkinsonism; Parkinson's Disease

Introduction

The primary pathology in Parkinson's Disease (PD) is a progressive loss of dopamine (DA) producing neurons originating in the midbrain's substantia nigra (SN), resulting in a progressive degeneration of projections of the SN to the striatum. This degeneration gives rise to clinical symptoms when approximately 50% dopaminergic cell loss in the SN is achieved, corresponding to an 80% depletion of striatal dopamine (Foley and Riederer, 1999). It has been proposed that during early stages of the illness, compensatory mechanisms, including increased neural activity by residual dopaminergic neurons and increased input from contralateral circuits and structures outside the basal ganglia, may be active (Bezard et al., 2003; Obeso et al., 2004). Consistent with these proposals is the clinical observation that patients during their disease learn to engage in alternative behavioral strategies that lead to a greater dependence on less compromised motor systems—an observation also noted in animal models of the disease (Lees, 1992; Schallert et al., 2000a,2000b).

To examine the question of reorganization of brain function, the current study used a rat model in which partial, unilateral striatal lesions were elicited with 6-hydroxydopamine. Such lesions have been shown to induce retrograde degenerative changes in the dopaminergic neurons of the substantia nigra that are progressive over the first few weeks after lesioning, with persistence of cell loss documented over 6-8 weeks (Cadet et al., 1991; Ichitani et al.,1994; Yuan et al., 2005), and relative sparing of the mesotelencephalic DA pathway (Sauer and Oertel, 1994). Our objective was to use functional brain mapping to investigate brain function with respect to (1) compensatory changes in regional cerebral activation in motor and nonmotor circuits, and (2) whether brain mapping performed during motor challenge can unmask underlying differences between normal and pathological neural circuits that are not apparent during the resting state.

Materials and methods

Animals

Adult, male Sprague-Dawley rats (250-275 g, Harlan Sprague-Dawley Labs, Indianapolis, IN, USA) were used under a protocol approved by the Animal Research Committee of the University of Southern California. Rats were housed in groups of 2 animals on a 12 h light: 12 h dark cycle (7 p.m.-7 a.m. lights off) with free access to water and rodent chow. Rats were trained over 2 weeks to run on the Rotarod treadmill (Columbus Instruments, Columbus, OH, USA), starting at a speed of 3.0 cm/s, progressing to 7.9 cm/s for 40 min/day by the 4th day, and continuing for 10 additional days.

Lesions

Animals were randomized to one of 4 groups: lesion + treadmill walking ($n = 9$), lesion + rest ($n = 9$), sham lesion + treadmill walking ($n = 8$) and sham lesion + rest ($n = 7$). Rats were placed under isoflurane anesthesia (1.3%) in a sterotaxic apparatus (Stoelting, Wood Dale, IL) and received injection of 6-OHDA (Sigma-Aldrich, St. Louis, MO) at two sites of the right striatum

(AP: 0.5, L: -2.5, V: -5.0 mm, and AP: -0.5, L: -4.2, V: -5.0 mm relative to bregma, with the tooth bar set at 0 mm). Injection was made at each site of 10 µg of 6-OHDA dissolved in 2 µl of 0.3% L-ascorbic acid/0.9% saline and administered at a rate of 0.5 µl/min using a 5-µl Hamilton microsyringe fitted with a 26 gauge, blunted needle. Sham-lesioned rats received injection of an equal volume of vehicle solution into the same two sites. After injection, the needle was left in place for 5 min before slowly retracting it. The cranial hole was sealed with dental cement and the skin sutured.

Assessment of neurological deficits

Three weeks after lesion surgery, rats were individually placed inside a spherically shaped Perspex bowl (Rotameter of 1 m diameter). Locomotor activity of the animals was recorded with a ceiling-mounted video camera. After recording a 10-min baseline, the rats received an intraperitoneal injection of D-amphetamine, an indirect dopaminergic agonist (5 mg/kg). The rat was placed back in the Rotameter and its locomotor activities were recorded for another 60 min. Data were analyzed off-line using Ethovision (Noldus Information Technology), a software package for behavioral analysis. Assessment was made of the total and net animal rotations (absolute and relative turns) during baseline and at different times after the D-amphetamine injection by analysis of variance with the repeated measure time and post-hoc t-tests ($p < 0.05$).

Implantation of a minipump

One week after the Rotameter testing, rats were anesthetized with isoflurane (1.3%). The ventral skin of the neck was aseptically prepared and the right external jugular vein was catheterized with a 5 French silastic catheter, advanced 3.5 cm into the superior vena cava. The catheter was tunneled through the subcutaneous space to the back and connected to a self-contained miniature infusion pump (MIP) situated subcutaneously in the infrascapular region.

Both the design of the MIP and its surgical implantation have been described in detail elsewhere (Holschneider et al., 2002; Moore et al., 2006). This pump allowed for unobtrusive intravenous bolus injection of the cerebral blood flow (CBF) tracer at the time of the brain mapping. The skin was sutured over the implant, except around the pump's percutaneous access port. The percutaneous port allowed for flushes of the catheter every 2 days postoperatively to ensure patency (0.8 ml of 0.9% saline, followed by 0.1 ml of 20 U/ml heparin in 0.9% saline). Following surgery, animals were individually housed.

Injection of the CBF radiotracer

Five days after implantation of the MIP, rats were immobilized for less than 5 min in a soft plastic rodent restrainer (Decapicone, Braintree Scientific, Braintree, MA) and the radiotracer ([^{14}C]-iodoantipyrine, 100 µCi/kg in 300 µl of 0.9% saline, American Radiolabelled Chemicals, St. Louis, MO), followed by a euthanasia agent (1 ml of 50 mg/ml pentobarbital, 3 M KCl), was loaded into the pump through a percutaneous port. Animals subsequently rested undisturbed for 40 min in a transport cage prior to exposure to the behavioral paradigm. Rats in treadmill walking groups were placed on the rotating cylinder (3.0 cm/sec) for 2 min. Rats in resting groups remained undisturbed in the transport cage while being exposed to the sound of the Rotarod.

We chose the Rotarod as an activational paradigm because it represents a strong motor challenge that involves motor exertion, limb coordination, balance and is free of negative conditioning inherent in paradigms that incorporate electric shock as an incentive for locomotion. The continuous nature of the locomotor paradigm allows for greater uniformity during the in-vivo circulation of the tracer. In this regard, it differs from a forelimb reaching task whose duration and execution may be variable. Furthermore, the Rotarod is preferred over

the horizontal treadmill in which side-to-side drifting of the rat can occur that would add potential variability to the functional imaging results. Exposure to the rotating rod prior to injection of the tracer was brief (2 min.) to avoid metabolic imbalances that may result as a result of extended exercise. A low walking speed was chosen to allow all animals to uniformly and easily perform the task without footslips or struggle.

The MIP was triggered transcutaneously by an infrared light source above the treadmill or transport cage. This resulted in bolus intravenous injection of the radiotracer, followed immediately by injection of the euthanasia solution. Cardiac arrest followed within ~10 s, accompanied by a precipitous fall of arterial blood pressure, termination of brain perfusion, and death (Holschneider et al., 2002). Brains were rapidly removed, flash frozen in dry ice/ methylbutane (-55 °C) and stored at -20 °C.

Autoradiography

Cerebral blood flow related tissue radioactivity (CBF-TR) was measured by the $[^{14}C]$-iodoantipyrine method (Goldman and Sapirstein, 1973; Sakurada et al., 1978; Patlak et al., 1984). In this method, there is a strict linear proportionality between tissue radioactivity and CBF when measurement is made within a brief interval (~10 s) after injection of the radiotracer (Van Uitert and Levy, 1978; Jones et al., 1991). Brains were sectioned in a cryostat at -18 °C in 20 μm sections, with an intersection spacing of 300 μm. At each bregma position duplicate sections were prepared. Sections were heat-dried on glass slides and exposed to Kodak Ektascan film for 15 days at room temperature with 16 $[^{14}C]$ standards (Amersham Biosciences). Images (autoradiographs) of brain sections were digitized on an 8-bit gray-scale with a ChromaPro 45 IAIS "Dumas" film illumination system and a Phillips charge-coupled device monochrome imaging module coupled to a Flashpoint 128 digitizing board on a microcomputer.

Statistical parametric mapping

Image alignment—The process of aligning slices to reconstruct the three dimensional (3D) brain, the spatial normalization and the smoothing of individual brains have been described in our earlier work (Nguyen et al., 2004). In brief, fifty-three digitized, serial coronal sections (bregma +4.2 mm to -11.2 mm, interslice distance 300 μm) were selected and stored as two-dimensional arrays of 72 μm^2 pixels. Adjacent sections were aligned both manually and using TurboReg (Thevenaz et al., 1998), an automated pixel-based registration algorithm (Nguyen et al., 2004).

Creation of the rat brain template—Individual 3D images were spatially normalized using a 12-parameter, nonlinear affine transformation into a standard space defined by a single, 'artifact free' rat brain, followed by a nonlinear spatial normalization using the low-frequency basis functions of the three-dimensional discrete cosine transform ($7 \times 7 \times 8$ in each direction for 1176 parameters), plus a linear intensity transformation (4 parameters) (Nguyen et al., 2004).

SPM analysis—Statistical Parametric Mapping (SPM) (Friston et al., 1990; Friston, 1995), which was introduced in 1991, (Wellcome Department of Cognitive Neurology, Institute of Neurology, London, UK), is a collection of tools available in the public domain for basic visualization and analysis of neuroimages (Nguyen et al., 2004; Lee et al., 2005). Our tracer injection, adapted for use in freely moving subjects, precluded the direct sampling of arterial blood necessary for obtaining quantitative measures of flow in ml/min-grams of brain tissue. Normalization was necessary to minimize intersubject variability, most importantly, differences in the total amount of tracer received by each animal. Global differences in the absolute amount of radiotracer delivered to the brain were adjusted by the SPM software in

each animal by scaling the voxel intensities so that the mean intensity for each brain was the same (proportional scaling). Voxels for each brain failing to reach a specified threshold (80%) were masked out to eliminate the background and ventricular spaces.

Using SPM, we implemented a Student t-test (unpaired) at each voxel ($72 \times 72 \times 300 \ \mu m^3$), testing the null hypothesis that there was no effect of group, i.e. no difference between [^{14}C]-iodoantipyrine CBF tracer distributions. Maps of positive and negative t were separately analyzed. A significance threshold was set at $p < 0.01$ (uncorrected for multiple comparisons) for individual voxels within clusters of contiguous voxels, and a minimum cluster size of 100 contiguous voxels (extent threshold). We then evaluated the corrected significance of individual voxels, clusters of contiguous voxels exceeding the threshold, and number of clusters detected in the entire SPM. Regions determined to be significant at the voxel level were required to show significance in two or more autoradiographic sections. Group differences in the distribution of CBF-TR were displayed as color-coded statistical parametric maps superimposed on the brain coronal, slices. Brain regions were identified using an anatomical atlas of the rat brain (Paxinos et al., 2005).

Region-of-interest analysis of cerebral cortex

Significant differences in the cerebral cortex (bregma +5.7 mm to -7.5 mm) were also examined using a region-of-interest (ROI) analysis, as previously reported (Holschneider et al., 2003). The optical density in a slice was measured within each hemisphere using custom software written in Matlab (The Mathworks Inc., Natick, MA). Regions in the cortex were sampled using a radial grid overlay, spaced in 15° intervals from the midline in a manner invariant between animals. Brain regions were identified using the anatomic atlas of the rat brain (Paxinos et al., 2005). Eight to 10 optical density measures were obtained per hemisphere along the cortical rim, as well as adjacent measures of background. Cortical structures included those listed in the legend of Fig. 3, as well as cingulate, prelimbic, and infralimbic cortex. A z-score transformation was performed on the tissue radioactivity data to produce patterns of regional cerebral blood flow tracer concentrations for each animal (Hays, 1973). This transformation eliminates variations in mean tracer distribution between subjects and experimental groups created by global effects on vascular smooth muscle and systematic experimental error. The topographic distribution of the CBF-related radioactivity (CBF-TR) on the dorsal, lateral, and basal cortical surfaces was displayed for every group as an anatomic map of the mean z-scores on the flattened cortex. Group differences in the z-scores of each ROI within each hemisphere were compared using t-tests (unpaired, two-tailed, $p < 0.05$). Laterality of the effects of lesioning were tested with a repeated measures analysis of variance using 'lesion' and 'treadmill walking' as the between subjects factors and the repeated measures 'hemisphere' and 'slice'. In addition to the analysis on the transformed data, analysis was also done on the nontransformed data for each location, each slice (all locations in a given slice) and globally (all locations in all slices).

Tyrosine hydroxylase immunohistochemistry

Duplicate brain sections were first fixed with acetone for 3 min, rinsed with Tris-Buffered Saline (TBS) and incubated at room temperature in blocking solution (10% normal goat serum/ PBS, DAB500 Kit, CHEMICON, Temecula, CA) for 10 min. Sections were then incubated for 3 h at room temperature with 1:400 solution of primary antibody (MAB 318, Mouse anti-tyrosine hydroxylase monoclonal antibody, CHEMICON) in a humidity chamber. Control sections were incubated in the blocking solution lacking primary antibodies. All sections were rinsed in TBS buffer and incubated for 10 min in the humidity chamber with a 1:200 solution of secondary antibody-HRP (Peroxidase Labeled Affinity Purified Antibody to Mouse IgG produced in Goat. Cat. 074-1806. KPL, Gaithersburg, MD). Finally sections were rinsed in TBS and incubated in a freshly prepared 3,3′ diaminobenzidine solution (DAB) for 3 min. DAB

reaction was terminated by TBS rinsing, sections were incubated with hematoxylin solution for 1 min and rinsed in TBS buffer again and dehydrated through a graded series of ethanol solutions and final xylene dip. Brain sections were mounted with xylene based mounting media, coverslipped, and viewed under bright field optics. The area distributed by tyrosine hydroxylase (TH)-positive fibers was measured in the striatum (AP +1.0 mm, -1.0 mm) and substantia nigra (AP -5.80 mm) using Image Pro-Plus software (Media Cybernetics, Silver Springs, MD). Significant group differences were analyzed by t-test (unpaired, two-tailed, $p < 0.01$).

Results

Lesions

Assessment of 6-OHDA lesion in striatal sections revealed a significant loss of dopaminergic fibers as indicated by a loss of TH-positive staining ($p < 0.0001$, Fig. 1). Lesion size at the level of the striatum as a percentage of the contralateral side was $39.4 \pm 4.3\%$ (AP +1.0 mm) and $27.5 \pm 5.2\%$ (AP -1.0 mm). By comparison, lesion size in the vehicle injected rats was respectively $0.2 \pm 1.8\%$ (AP +1.0 mm) and $0.4 \pm 2.0\%$ (AP -1.0 mm). Retrograde dopaminergic cell losses were also apparent in the substantia nigra, ipsilateral to the striatal lesion, with greatest losses noted in the pars compacta. Lesion size at -5.8 mm posterior to bregma was $35.0 \pm 3.1\%$ and $0.2 \pm 1.5\%$ for the 6-OHDA and vehicle injected rats, respectively. In agreement with prior work, no difference was noted in the TH staining intensity between lesioned and sham-lesioned rats at the level of the striatum or substantia nigra contralateral to the injection site (Roedter et al., 2001). The loss of TH staining was slightly lower in our study than that reported in other studies using similar doses of the toxin. Such differences may have been due to the prelesion training on the Rotarod, which may offer some neuroprotection to subsequent brain lesioning (Cohen et al., 2003).

Changes of rotational activity after amphetamine challenge

Significant differences in total, as well as net rotation were seen between the lesion and sham-lesion groups at baseline (Fig. 2), with lesioned rats (but not sham-lesioned rats) exhibiting rotational asymmetry in the direction towards the lesioned side. This rotational asymmetry increased progressively after administration of amphetamine (5 mg/kg, i.p.), peaking 40 min after injection (Time × Lesion, $F_{6,26} = 7.89$, $p < 0.0005$).

ROI analysis of cortical perfusion

Lesions resulted in changes in the cerebral blood flow tracer distribution (CBF-TR) over the lesioned hemisphere (Hemisphere × Lesion, $F_{1,326} = 4.3$, $p < 0.039$), with lateralized differences at specific anterior-posterior levels (Hemisphere × Slice × Lesion, $F_{44,283} = 2.4$, $p < 0.0005$), and lateralized differences at specific anterior-posterior levels in response to treadmill walking (Hemisphere × Slice × Lesion × Treadmill, $F_{44,283} = 1.4$, $p < 0.030$).

Rest—Sham-lesioned rats revealed their highest CBF-TR in primary somatosensory cortex mapping the barrel field (S1BF), jaw and upper lip region (S1J, S1U), secondary somatosensory cortex (S2), anterior-medial aspects of the auditory cortex (Au), and anteriorlateral portions of visual cortex (V2). Lowest regional z-scores were seen in the cortical amygdala (A), lateral entorhinal (LEnt), posterior perirhinal (PRh), retrosplenial (RSA), and posterior piriform cortex (Pir). This topographic pattern (data not shown) was similar to that described previously in the normal, awake, restrained rat (Holschneider and Scremin, 1998; Waite et al., 1999).

At rest, lesioned compared to sham-lesioned rats showed significantly greater CBF-TR (Table 1A, Fig. 3), bilaterally in primary and secondary motor cortex (M1, M2, range: $p < 0.05$ to <0.005), primary somatosensory cortex of the hind- and forelimbs, as well as parietal cortex

(S1HL, S1FL, P, range: $p < 0.05$ to <0.001). Significant increases in CBF-TR in M1 and M2 were more broadly represented in the contralateral than ipsilateral hemisphere, and extended anteriorly to include portions of frontal association cortex (FrA, $p < 0.01$), and posteriorly to somatosensory cortex of the trunk and to the retrosplenial cortex (S1Tr, RS, range: $p < 0.05$ to 0.01). Lesioned compared to sham-lesioned rats showed decreased CBF-TR bilaterally in insular, olfactory, amygdaloid cortex and the perirhinal/lateral entorhinal transition region (I, O, A, PRh/LEnt, range: $p < 0.05$ to <0.001).

Motor challenge—Sham-lesioned rats (Table 1D) showed significant bilateral activation in response to treadmill walking in M1 and M2 (range: $p < 0.02$ to <0.001), in S1HL, S1FL, S1Tr, and in primary somatosensory cortex mapping the shoulder (S1S)(range: $p < 0.01$ to <0.001), in medial portions of FrA (range: $p < 0.05$ to <0.005), and in secondary visual cortex and retrosplenial cortex (V2, RS, range: $p < 0.05$ to <0.01). Significant decreases in CBF-TR appeared in somatosensory cortex mapping the jaw and upper lip region (S1J, S1U), lateral portions of S1BF and lateral portions of FrA and piriform cortex (range: $p < 0.05$ to <0.001). This topography of activation was similar to that previously reported by our group in normal rats during treadmill walking (Holschneider et al., 2003;Nguyen et al., 2004). Small differences were noted, in particular an increases in CBF-TR in FrA, an anterior area of brain not sampled in our prior publication. Also noted in the current study was a bilateral increase in the posterior PRh/LEnt cortex, which reached statistical significance only on the right. A similar asymmetry, though over a more restricted area of PRh/LEnt, was observed in our earlier study.

Lesioned rats showed a similar pattern of activation in response to treadmill walking in M1 and M2 (range $p < 0.05$ to <0.001), and in S1FL, S1HL, S1Tr, and S1S (range $p < 0.05$ to <0.001) (Table 1C). However, compared to sham-lesioned rats (Table 1B), the magnitude of the CBF-TR increases ipsilaterally in M1 and M2 were significantly less in the lesioned animals. Also attenuated over the lesioned hemisphere were the locomotor-induced increases in CBF-TR in FrA and S1FL. The only cortical region demonstrating increased CBF-TR ipsilaterally during treadmill walking in the comparison between lesioned versus sham-lesioned rats was parietal cortex (P). In contrast, in the contralateral hemisphere increases in CBF-TR in response to treadmill walking were greater in FrA, M1, M1/M2 transition cortex, P, RS, S1BF, S1FL, S1S, S1Tr, S1UL, and V1 in lesioned than in sham-lesioned rats (range $p < 0.05$ to <0.005, Table 1B). There were no statistical differences between the locomotor and rest groups in non-transformed cortical CBF-TR or z-scores of CBF-TR calculated by slice or globally across all cortical regions.

SPM whole brain analysis

Significant group differences in CBF-TR obtained after statistical parametric mapping are shown in the form of T-score differences mapped onto select coronal sections of the rat brain (Fig. 4). A comprehensive list of significant group differences is shown in Table 2. Results are more fully discussed in their anatomic and clinical context in the discussion below.

Discussion

Based on the immunohistochemical and behavioral findings, lesions in our study fell within the scope of so-called 'moderate and compensated' lesions (Schwarting et al., 1996). Moderate and compensated lesions, while showing decreased input from the striatum to the substantia nigra via direct or indirect pathways, may demonstrate increased activity of both residual ipsilateral dopaminergic neurons, recruitment of alternate circuits, as well as increased input from the contralateral side. This may provide a relatively 'normal' level of innervation to the neostriatum. Such compensations have been shown to occur at the level of increased transmitter

synthesis, impulse-flow and release, decreased transmitter re-uptake and spontaneous turning behavior (reviewed in Schwarting and Huston, 1996a,1996b; Schwarting et al., 1996).

Functional brain activation after nigrostriatal lesions

Two prior studies have demonstrated no change in absolute CBF in the awake, restrained rat in the striatum, SN, cortex and a number of brain areas, 2 weeks after 6-OHDA lesions of the left SN (Dahlgren et al., 1981; Lindvall et al., 1981). Another study performing lesions of the right SN and ventral tegmental area, however, found a decrease in CBF in the ipsilateral neostriatum and amygdala, but not in the cortex (Mraovitch et al., 1993). Such discrepancies may be ascribable to differences in the extent of lesion, the lesion sites or laterality. More consistent have been reports about lateralized changes in local blood flow elicited under stimulated conditions, for example when using dopaminergic challenges like amphetamine or apomorphine (Lindvall et al., 1981; Harik et al., 1982; Ingvar et al., 1983). Our study evaluated CBF after 5 weeks following lesioning of the striatum at two anterior-posterior coordinates. In addition to a more detailed ROI analysis, we used a novel, voxel-based 3-D imaging analysis which was not restricted to typical boundaries inherent to the ROI approach. Using these tools, we were able to show the following significant changes in relative perfusion at rest and during a locomotor challenge.

Ipsilateral brain—At rest, lesioned compared to sham-lesioned rats showed increased functional activity in the cerebral cortex, mostly in motor and somatosensory areas. At the same time, there was a robust hyperemia in white matter fiber tracts responsible for intra-, as well as interhemispheric information transfer (anterior commissures, corpus callosum, external capsule, forceps minor and major). Such increases suggest a compensatory mechanism by which residual cells overcome deficits related to a partial deafferentation of the striatofrontal projections. Significant increases were also noted in several parts of the motor circuit (internal globus pallidus, subthalamic nucleus, anterior substantia nigra, ventral lateral, ventral anterior thalamus), and the ventral posterolateral (VPL) nucleus of the thalamus (discussed below).

The hyperemia noted at rest, however, could not compensate sufficiently under conditions of a locomotor challenge. Treadmill walking unmasked ipsilateral hypoperfusion in motor cortex (M1, M2), somatosensory cortex (S1FL, S1U), the striatum, and globus pallidus (internal, external). During the motor challenge lesioned compared to sham-lesioned rats also diminished their CBF-TR in the intra- and inter- hemispheric white matter tracts. Decreases were most marked ipsilateral to the lesion, but were also seen contralaterally and across the midline. The only significant cortical increase noted was in parietal cortex, which has been associated with processing of spatial information (Kolb et al., 1983; DiMattia and Kesner, 1988) and shows increased perfusion during performance of manual finger tasks in patients with PD (Samuel et al., 1997; Catalan et al., 1999). Subcortical increases in CBF-TR included the red nucleus, superior colliculus, and thalamus (ventroposterior lateral, ventromedial), with no activation noted in the ipsilateral STN.

Contralateral brain—Though corticostriatal pathways are dominantly ipsilateral, substantial crossed projections exist across the anterior corpus callosum (Dunnett et al., 2005). In addition, there is histologic evidence (Morgan and Huston, 1990) for interhemispheric projections from the substantia nigra to the striatum, and electrophysiological evidence that activity in nigrostriatal dopaminergic cells (Castellano and Rodriguez Diaz, 1991), as well as in the STN (Perier et al., 2000a,2000b) are under control of the contralateral brain. There appears to be functional and, at least in part, compensatory interdependence of the two nigrostriatal systems, since unilateral manipulations (lesioning or stimulation) of one nigrostriatal system affect contralateral DA turnover, DA synthesis, and alterations in dopaminergic D1:D2 receptor interactions (reviewed in Schwarting et al., 1996; Roedter et al.,

2001). Such projections may provide for the interhemispheric coordination of basal ganglia activity.

At rest, lesioned rats showed increased CBF-TR in contralateral cerebral cortex, mostly in motor, somatosensory and parietal cortex. Different from the ipsilateral findings was the recruitment of a broader area of primary somatosensory cortex (S1FL, S1Sh, S1J, S1U) and frontal association cortex. At the same time, there was a robust hyperemia in contralateral white matter fiber tracts responsible for intra-, as well as interhemispheric information transfer, though somewhat less so than ipsilateral to the lesion. Also, there was a small but significant increase in the CBF-TR of the STN.

The locomotor challenge elicited a hyperemia in the contralateral cortex in the lesioned compared to the sham-lesioned rats. Significant increases were noted in the recruitment of somatosensory cortex (S1BF, S1FL, S1J, S1S, S1Tr, S1U), motor, parietal, frontal association and retrosplenial cortex. Of note, lesioned compared to sham-lesioned rats demonstrated a broadening of the cortical sensorimotor map at rest and during treadmill walking. Such a 'diffusion' or remapping of cortical sensorimotor activity has been previously reported in the unilateral PD animal model (Pelled et al., 2002; Metz et al., 2004). At the same time, the increased demands elicited by the motor task, resulted in increased recruitment in the contralateral STN, anterior SN, red nucleus and zona inserta. Thus, the increase in CBF-TR in the STN was noted to a small extent bilaterally at rest, and dramatically, and only contralaterally, during treadmill walking. This finding is of interest in so far as the STN represents a key region in the indirect pathway within the basal ganglia circuitry (discussed below). Inputs to the red nucleus (RPC) include the sensorimotor cortex, cerebellar nuclei, and zona incerta and the RPC is believed to play a role in intra- and interlimb coordination of movement (Lavoie and Drew, 2002; Hermer-Vazquez et al., 2004; Ruigrok, 2004). The zona inserta with projections to the basal ganglia (Heise and Mitrofanis, 2004) is hyperactive in 6-OHDA-lesioned rats (Perier et al., 2000a,2000b) and has been the target of deep brain stimulation to improve symptoms of bradykinesia in PD subjects (Henderson et al., 2002; Voges et al., 2002).

Increased CBF-TR was also noted in lesioned compared to sham-lesioned rats in the ventromedial thalamic nucleus (VM) and the ventral subiculum (VS) during the locomotor challenge. The VM is in general considered to be part of the motor thalamus. Subcortical inputs to the VM originate to a large degree in the internal segment of the globus pallidus and the substantia nigra (nigrothalamic pathway). Afferents from the cerebellum have also been identified. Projections from the VM reach widespread cortical areas, in particular in the rostral, frontal part of the hemisphere and include motor cortex (thalamo-cortical pathway). Lesions of the VS have been previously linked with alterations in locomotor responsiveness to amphetamine (Burns et al., 1996; Taepavarapruk et al., 2000; Caine et al., 2001). Electrical stimulation of the VS evokes hyperlocomotion and increased dopamine efflux in the rat nucleus accumbens (Taepavarapruk et al., 2000). It has been suggested that the VS may play a role in the initiation of locomotor movement (Ma et al., 1998).

Midline brain—During the resting state, lesioned compared to sham-lesioned rats demonstrated small but significant increases in CBF-TR in the midline cerebellum, which were dramatically enhanced during treadmill walking. Past work has shown that stimulation of the forelimbs and hindlimbs elicits extracellular recorded responses in the vermis of lobules 2 to 7 (Saint-Cyr and Woodward, 1980; Santori et al., 1986), and Rotarod walking increases c-*fos* expression in these vermal lobules (Jasmin et al., 1994) (but see also (Ruigrok et al., 1996)). In addition, anterograde autoradiography and retrograde horseradish peroxidase methods have revealed that the vermal and paravermal lobules are targets of the dorsal column-lemniscal system which provides somatosensory information from the spinal cord. CBF-TR

was also greater in lesioned compared to sham-lesioned rats in the central medial thalamic nucleus and septal nuclei (lateral intermediate medial, triangular, septofimbrial). While the central medial nucleus, at least in its caudal portion, projects widely to motor and sensory cortex (Groenewegen et al., 2004), the septal nuclei have been reported to show evidence of TH staining (Risold and Swanson, 1997) and dopaminergic fibers (Taghzouti et al., 1985).

Motor challenge also increased CBF-TR in the supramammillary nucleus (SuM). The supramammillary nucleus contains many dopaminergic neurons (Swanson, 1982), some of which are extensions of the A10 cell group (ventral tegmental area), which shows a decrease in tyrosine hydroxylase staining cells after striatal lesions (Yuan et al., 2005). The SuM has projections to the lateral septum and plays a prominent role in the modulation of the theta rhythm (Pan and McNaughton, 2004). One may speculate that increases in dopaminergic neuronal activity in the supramammillary nucleus may serve to increase synchronized afferent activity to drive SN oscillations which may be disrupted after 6-OHDA lesions (Meissner et al., 2006).

Striato-pallidal pathways

The classic view of basal ganglia connections is based upon the identification of two distinct striato-pallidal pathways (Fig. 5) (Albin et al., 1989;Alexander et al., 1990). Though this model is currently recognized to represent a simplification of the neural circuitry (Obeso et al., 2000), in it a 'direct' pathway leads from the striatum straight to the globus pallidus pars interna (GPI) and other basal ganglia output nuclei, while an 'indirect' pathway first transmits to the globus pallidus pars externa (GPE) and the STN. A prediction of the direct-indirect pathways model is that the akinesia associated with Parkinson's disease is due to an imbalance in activity in the two pathways in favor of the indirect pathway (Albin et al., 1989;Bergman et al., 1990;DeLong, 1990). More specifically, in the indirect pathway GABAergic inhibitory efferents from the striatum to the GPE are proposed to be overactive. This increased inhibition of the GPE results in a disinhibition of the STN and, thus, overactivity of basal ganglia outputs from the GPI and the substantia nigra reticulate (SNr). Lesioning of the striatum also results in increased activity at the level of the GPI/SNr through decreased inhibitory influence from GABAergic projections from the striatum itself (direct pathway). Such increases in neuronal activity of the GPI/SNr should result in increased inhibition of the VL/VA, with resultant decreased activity in sensorimotor cortex.

Consistent with the classic view, our study showed a significant increase in CBF-TR in the STN of lesioned compared to sham-lesioned animals, suggesting a modest bilateral basal hyperactivity. That such increases are compensatory has been suggested by observations that blockade of the STN excitation of surviving DA neurons in the presymptomatic period of the MPTP-primate model of PD can provoke the emergence of parkinsonian symptoms (Bezard et al., 1997). Also consistent with the classic view, was the increased CBF-TR at rest in the lesioned compared to sham-lesioned animals in the ipsilateral GPI and a decrease or no change in CBF-TR in the striatum and GPE. However, contrary to the classic view, we saw increases at rest in CBF-TR in the ipsilateral VL, VA and bilateral motor cortex. At the same time, CBF-TR was increased in the white matter tracks within and between hemispheres. These findings are in line with recent experimental results showing bilateral overactivation of the sensorimotor cortex in the unilateral rodent model of PD (Pelled et al., 2002). Such cortical hyperactivity is difficult to explain using the classical model of basal ganglia function (Alexander et al., 1990), which are based largely on primate anatomy. Furthermore, this model does not address interhemispheric interactions as might result from direct strong corticocortical connections of the hemispheres through the corpus callosum; contralateral connections between the basal ganglia and the cortex, and/or possibly connections between the VM and cortex.

Findings during the locomotor challenge differed from those at rest. Ipsilaterally there was a deactivation or absence of activation across the striato-pallidal-thalamic-cortical circuit. Contralaterally, however, we saw increases in CBF-TR in both the STN, anterior SN, and motor cortex.

Somatosensory circuits—In addition to motor deficits, the rat model of unilateral 6-OHDA lesions has been documented to display somatosensory 'hyperreactivity' for tactile stimulation ipsilateral to the lesion, while sensory neglect is seen contralateral to the lesion (Schwarting et al., 1996). Likewise, preliminary work has shown that patient's with PD have altered sensory processing to a vibratory stimulus, with both increases and decreases in brain functional brain activation within the somatosensory system (Boecker et al., 1999). Such findings have suggested the presence of either altered central focusing and gating of sensory impulses, or enhanced compensatory recruitment of associative sensory areas in the presence of basal ganglia dysfunction. Thus, brain lesioning likely altered not only motor output from the brain during treadmill walking, but also afferent input from the somatosensory system that provided tactile and proprioceptive information from the animal's body.

Lesioned compared to sham-lesioned rats showed bilateral increases in CBF-TR of the somatosensory cortex at rest and contralaterally in response to the locomotor challenge. Such increases suggest that somatosensory cortex may have to 'work harder' after striatal damage in order to provide adequate sensory processing to the animal, both at rest and during treadmill walking. As noted above, the increases contralaterally suggest presence of a compensatory recruitment of neurons that may be operating via corticocortical and transcallosal connections, or else via contralateral connections between the basal ganglia and the cortex.

Also increased at rest was the CBF-TR in the ventral posterolateral (VPL) nucleus of the thalamus. Increases were noted ipsilaterally at rest and bilaterally during the locomotor challenge. The VPL is a primary thalamic relay for somatic sensory, i.e. tactile/kinesthetic and nociceptive information from the trunk and limbs (Groenewegen et al., 2004), which provides direct projections to the caudal striatum (Erro et al., 2001). Increased perfusion in the VPL may indicate increased neural activity whose aim is to boost neural input to a hypofunctional striatum.

The CBF-TR patterns in response to treadmill walking in the sham-lesioned animals, also revealed significant changes in several regions within the ascending dorsal column-lemniscal system. This system sends ascending fibers from the spinal cord's gracilis nucleus and cuneate nuclear complex to the midbrain and cerebellum, providing tactile, as well as proprioceptive information from all parts of the body (Graybiel, 1972) (Massopust et al., 1985). In our study, significant changes within this system were noted in sham-lesioned rats in response to the locomotor challenge, included the lateral lemniscus (decrease), inferior colliculus (decrease), superior colliculus (decrease), medial geniculate (decrease), pretectal nuclei (decrease), cerebellar vermis (increase), and ventroposterior lateral thalamus (decrease). Consistent with the notion of enhanced compensatory recruitment within the dorsal column-lemniscal system after striatal injury, we found significant increases in CBF-TR between lesioned and sham-lesioned animals during treadmill walking, bilaterally in the VPL, contralaterally in the lateral lemniscus, as well as in the cerebellar vermis.

Functional neuroimaging in normal subjects and PD patients during motor activation

Brain mapping performed during motor challenges has been previously reported in early PD, though these have typically used manual finger tasks rather than walking. In agreement with the classic PD model, numerous imaging studies using PET have shown cortical hypoactivation in motor-related areas in human PD subjects performing simple motor tasks, compared with normal subjects (Jenkins et al., 1992; Playford et al., 1992; Jahanshahi et al., 1995). However,

other studies have found increased neuronal activity in different regions of the motor, frontal and sensory cortices in parkinsonian patients (Boecker et al., 1999; Sabatini et al., 2000), and electrophysiological studies of single neurons in a monkey model of PD reported no change in the mean spontaneous primary motor cortex discharge (Doudet et al., 1990; Goldberg et al., 2002). Such differences have been explained on methodologic grounds and by differences in the severity of PD between subjects studied. Comparison of these studies to our study is complicated by the fact that PD, though it may show asymmetry, typically is a bilateral disease of the nigrostriatal system, whereas our animals received unilateral lesions. Nevertheless, these studies make several points which parallel the results of our work: (a) functional brain activation during a motor challenge unmasks underlying differences between normal and pathological neural circuits that are not apparent at rest (Jenkins et al., 1992; Playford et al., 1992; Rascol et al., 1994, 1997; Jahanshahi et al., 1995; Samuel et al., 1997), with hypoperfusion noted in premotor, prefrontal and supplemental motor cortex and the putamen; (b) performance of a unimanual task elicits activation of ipsilateral motor cortex in PD subjects but not in controls (Rascol et al., 1994, 1998; Thobois et al., 2000)— activation that requires interhemispheric neural input; (c) Compensation for striatal dysfunction can occur through recruitment of nonmotor cortex, including parietal cortex (Samuel et al., 1997; Catalan et al., 1999), (d) Motor challenge in PD subjects elicits activation of the cerebellum not apparent in elderly, control subjects (Rascol et al., 1997; Hanakawa et al., 1999; Albani et al., 2001). Enhanced cerebellar activation in the vermis was noted in the only human study to date that examined PD patients during treadmill walking using SPECT (Hanakawa et al., 1999).

Imaging studies of PD patients with asymmetric motor symptoms (hemiparkinsonism) have shown that during the execution of a motor task with a non-akinetic hand, cerebral activation in PD patients appeared similar to that of controls (Thobois et al., 2000). Activated areas were the primary motor cortex, premotor cortex, parietal cortex and cerebellum. This suggests that a significant degree of akinesia is necessary to induce an abnormal pattern of cerebral activation during a motor task. However, when these subjects engaged in the same motor task with their akinetic hand, ipsilateral activation of primary motor cortex was noted. Such ipsilateral activations were noted even when patients were off drugs, had no dyskinesia and no significant tremor at the time of the PET studies. Similarly, two SPECT studies have demonstrated bilateral activation of primary motor cortex during a unimanual motor task in PD patients (Rascol et al., 1994, 1998). Such findings could represent a presymptomatic rCBF overactivation which itself is insufficient to induce involuntary movements. Alternatively it may represent the recruitment of accessory motor pathways in order to compensate for the dysfunction of the basal ganglia.

That differences in neural activation, overactivation, or no response in PD patients performing motor tasks may relate to the relative magnitude of dopaminergic tone was suggested amongst others by Rascol et al. (Rascol et al., 1992). Here imaging sequential finger movements using SPECT demonstrated that PD subjects with akinesia, unlike normal controls, showed no change in CBF in the supplementary motor areas and in the contralateral primary sensory motor cortex. However, these deficits were reversed when PD patients in the 'off' state were converted to the 'on' state by a subcutaneous injection of apomorphine, a DA receptor agonist. These results suggest a functional deafferentation of the cortical motor areas in PD subjects—an abnormality that can in part be reversed by dopaminergic drugs. Our study suggests that functional deafferentation can also be countered during a treadmill challenge by increased activation of motor circuits in the contralateral brain, as well as the recruitment of alternate brain regions. That this activation may result from increases in dopamine release is suggested by microdialysis studies which have shown that exercise acutely increases the concentration of DA in the striatum of the rat (Sabol et al., 1990; Hattori et al., 1994).

Basal ganglia circuits in rodent and human locomotion

Rat and human basal ganglia share many features. They both demonstrate the existence of dorsal and ventral striatopallidal systems, striatonigral and nigrostriatal projections, and descending pathways from the striatopallidal system to the midbrain tectum and reticular formation. The connectional similarities are paralleled by similarities in the general distribution of chemical markers of striatal and pallidal structures such as dopamine, substance P and enkephalin, as well as by similarities in development (Medina and Reiner, 1995; Smeets et al., 2000; Hardman et al., 2002). Nevertheless, substantial differences exist between rat and human basal ganglia which may reflect differences in aspects of behavior, and in susceptibility to developing PD symptoms. (Smeets et al., 2000). Such differences could in principle also modify the compensatory response elicited after cell loss in the nigrostriatal system. For instance, there are differences in the proportional volume of individual brain structures, differences in the anatomic distribution of TH+ neurons within the dopaminergic SN, and differences in the anatomic continuity of the GPI and GPE (Hardman et al., 2002). Basal ganglia output in rats has been reported to be concentrated in pathways emanating from the nondopaminergic SN (SNND). Conversely, humans have fewer developed SNND neurons (and less output neurons overall) and larger overall proportions of STN and GPE neurons compared with rats, suggesting greater internal basal ganglia regulation of information before output through the GPI and SNND (Hardman et al., 2002). Furthermore, there are interspecies differences in the morphology of dopaminergic SN neurons, which may result in differences in input resistance and firing patterns between primates and rats (Kotter and Feizelmeier, 1998).

Although quadrupedal gait may in principle involve activation of different neural circuits when compared to bipedal gait, the current study and our previous work mapping CBF during treadmill walking in normal rats has shown that this task engages motor circuits, primary somatosensory cortex mapping the forelimbs, hindlimbs and trunk, as well as secondary visual cortex (Holschneider et al., 2003; Nguyen et al., 2004). These results concur with work in humans that demonstrates during walking increases of regional CBF in the supplementary motor area, medial primary sensorimotor area, visual cortex, striatum, visual cortex and the cerebellar vermis using single photon emission computed tomography (SPECT)(Fukuyama et al., 1997; Hanakawa et al., 1999).

Limitations

A limitation to the current study was that in addition to dopaminergic neurons, 6-OHDA can to some extent also be taken up into and destroy other catecholaminergic neurons. The extent of involvement of nondopaminergic neurons is dependent on the site and (less so) on toxin amount (Schwarting et al., 1996). Changes we observed in functional brain activation may have been initiated not simply by dopaminergic deficits and their downstream consequences, but also by, for instance, changes in noradrenaline and/or serotonin. Such issues notwithstanding, neuronal damage in PD is also not selective for dopamine, but includes to some extent changes in noradrenaline (Gesi et al., 2000) and serotonin (Nicholson and Brotchie, 2002) as well.

Although the existence of a flow/metabolism coupling at rest is well accepted, the exact relationship between neuronal activity, regional CBF, and metabolism during cerebral activation remains a question of debate (Gsell et al., 2000; Keri and Gulyas, 2003). Unresolved issues include (a) the assumption that behavioral performance shows correlations with regional CBF equally in all brain regions, (b) the limits of proxy measures such as regional CBF have in detecting changes in spatial and temporal neural processing, in which the overall energy demands may remain unchanged, and (c) the role of excitatory compared to inhibitory neurotransmitters have in altering brain perfusion and metabolism. In particular, hemodynamic

changes evoked by activation can be driven by subthreshold synaptic activity. The balance between synaptic excitation and inhibition, as well as the electroresponsive properties of the targeted nerve cells themselves, controls the amplitudes of the neuronal and vascular signals. Hence, it is not possible on the basis of an increase in regional CBF to definitively judge whether the output or input activity of that region is increased or whether such activity represents changes in inhibitory or excitatory activity.

Summary

Our results showed that following partial unilateral damage of the nigrostriatal system that (a) functional brain activation differed at rest and during treadmill walking, with ipsilateral deficits in the striato-pallidal-thalamic-cortical circuit most apparent during the locomotor challenge, (b) a number of compensatory changes in motor areas were noted outside the classic striato-pallidal circuitry, (c) functional compensations were noted in both hemispheres, but during the locomotor challenge were mostly contralateral and in midline cerebellum, and (d) there was enhanced compensatory recruitment of associative sensory areas in both cortex and subcortex. Future models of compensatory changes in motor circuits after damage to the nigrostriatal system should address the effects of increased neural activity by residual dopaminergic neurons, interhemispheric interactions and that compensation may differ between resting and locomotor states.

Acknowledgements

References

Albani G, Kunig G, Soelch CM, Mauro A, Priano L, Martignoni E, Leenders KL. The role of language areas in motor control dysfunction in Parkinson's disease. Neurol. Sci 2001;22:43–44. [PubMed: 11487193]

Albin RL, Young AB, Penney JB. The functional anatomy of basal ganglia disorders. Trends Neurosci 1989;12:366–375. [PubMed: 2479133]

Alexander GE, Crutcher MD. Functional architecture of basal ganglia circuits: neural substrates of parallel processing. Trends Neurosci 1990;13:266–271. [PubMed: 1695401]

Alexander GE, Crutcher MD, DeLong MR. Basal ganglia-thalamocortical circuits: parallel substrates for motor, oculomotor, "prefrontal" and "limbic" functions. Prog. Brain Res 1990;85:119–146. [PubMed: 2094891]

Bergman H, Wichmann T, DeLong MR. Reversal of experimental parkinsonism by lesions of the subthalamic nucleus. Science 1990;249:1436–1438. [PubMed: 2402638]

Bezard E, Boraud T, Bioulac B, Gross CE. Presymptomatic revelation of experimental parkinsonism. NeuroReport 1997;8:435–438. [PubMed: 9080424]

Bezard E, Gross CE, Brotchie JM. Presymptomatic compensation in Parkinson's disease is not dopamine-mediated. Trends Neurosci 2003;26:215–221. [PubMed: 12689773]

Boecker H, Ceballos-Baumann A, Bartenstein P, Weindl A, Siebner HR, Fassbender T, Munz F, Schwaiger M, Conrad B. Sensory processing in Parkinson's and Huntington's disease: investigations with 3D H(2)(15)O-PET. Brain 1999;122(Pt 9):1651–1665. [PubMed: 10468505]

Burns LH, Annett L, Kelley AE, Everitt BJ, Robbins TW. Effects of lesions to amygdala, ventral subiculum, medial prefrontal cortex, and nucleus accumbens on the reaction to novelty: implication for limbic-striatal interactions. Behav. Neurosci 1996;110:60–73. [PubMed: 8652073]

Cadet JL, Last R, Kostic V, Przedborski S, Jackson-Lewis V. Long-term behavioral and biochemical effects of 6-hydroxydopamine injections in rat caudate-putamen. Brain Res. Bull 1991;26:707–713. [PubMed: 1933391]

Caine SB, Humby T, Robbins TW, Everitt BJ. Behavioral effects of psychomotor stimulants in rats with dorsal or ventral subiculum lesions: locomotion, cocaine self- administration, and prepulse inhibition of startle. Behav. Neurosci 2001;115:880–894. [PubMed: 11508727]

Castellano MA, Rodriguez Diaz M. Nigrostriatal dopaminergic cell activity is under control by substantia nigra of the contralateral brain side: electrophysiological evidence. Brain Res. Bull 1991;27:213–218. [PubMed: 1742610]

Catalan MJ, Ishii K, Honda M, Samii A, Hallett M. A PET study of sequential finger movements of varying length in patients with Parkinson's disease. Brain 1999;122(Pt 3):483–495. [PubMed: 10094257]

Cohen AD, Tillerson JL, Smith AD, Schallert T, Zigmond MJ. Neuroprotective effects of prior limb use in 6-hydroxydopamine-treated rats: possible role of GDNF. J. Neurochem 2003;85:299–305. [PubMed: 12675906]

Dahlgren N, Lindvall O, Nobin A, Stenevi U. Cerebral circulatory response to hypercapnia: effects of lesions of central dopaminergic and serotoninergic neuron systems. Brain Res 1981;230:221–233. [PubMed: 6797677]

DeLong MR. Primate models of movement disorders of basal ganglia origin. Trends Neurosci 1990;13:281–285. [PubMed: 1695404]

DeLong MR, Wichmann T. Circuits and circuit disorders of the basal ganglia. Arch. Neurol 2007;64:20–24. [PubMed: 17210805]

DiMattia BV, Kesner RP. Role of the posterior parietal association cortex in the processing of spatial event information. Behav. Neurosci 1988;102:397–403. [PubMed: 3395449]

Doudet DJ, Gross C, Arluison M, Bioulac B. Modifications of precentral cortex discharge and EMG activity in monkeys with MPTP-induced lesions of DA nigral neurons. Exp. Brain Res 1990;80:177–188. [PubMed: 1972680]

Dunnett SB, Meldrum A, Muir JL. Frontal-striatal disconnection disrupts cognitive performance of the frontal-type in the rat. Neuroscience 2005;135:1055–1065. [PubMed: 16165288]

Erro ME, Lanciego JL, Arribas J, Gimenez-Amaya JM. Striatal input from the ventrobasal complex of the rat thalamus. Histochem. Cell Biol 2001;115:447–454. [PubMed: 11455444]

Foley P, Riederer P. Pathogenesis and preclinical course of Parkinson's disease. J. Neural Transm., Suppl 1999;56:31–74. [PubMed: 10370902]

Friston KJ. Commentary and opinion: II. Statistical parametric mapping: ontology and current issues. J. Cereb. Blood Flow Metab 1995;15:361–370. [PubMed: 7713993]

Friston KJ, Frith CD, Liddle PF, Dolan RJ, Lammertsma AA, Frackowiak RS. The relationship between global and local changes in PET scans. J. Cereb. Blood Flow Metab 1990;10:458–466. [PubMed: 2347879]

Fukuyama H, Ouchi Y, Matsuzaki S, Nagahama Y, Yamauchi H, Ogawa M, Kimura J, Shibasaki H. Brain functional activity during gait in normal subjects: a SPECT study. Neurosci. Lett 1997;228:183–186. [PubMed: 9218638]

Gesi M, Soldani P, Giorgi FS, Santinami A, Bonaccorsi I, Fornai F. The role of the locus coeruleus in the development of Parkinson's disease. Neurosci. Biobehav. Rev 2000;24:655–668. [PubMed: 10940440]

Goldberg JA, Boraud T, Maraton S, Haber SN, Vaadia E, Bergman H. Enhanced synchrony among primary motor cortex neurons in the 1-methyl-4-phenyl-1,2,3,6-tetrahydropyridine primate model of Parkinson's disease. J. Neurosci 2002;22:4639–4653. [PubMed: 12040070]

Goldman H, Sapirstein LA. Brain blood flow in the conscious and anesthetized rat. Am. J. Physiol 1973;224:122–126. [PubMed: 4566847]

Graybiel AM. Some fiber pathways related to the posterior thalamic region in the cat. Brain Behav. Evol 1972;6:363–393. [PubMed: 4662203]

GroenewegenHJWitterMP Thalamus, G. Paxinos, The Rat Nervous System2004407453Elsevier Academic PressSan Diego

Gsell W, De Sadeleer C, Marchalant Y, MacKenzie ET, Schumann P, Dauphin F. The use of cerebral blood flow as an index of neuronal activity in functional neuroimaging: experimental and pathophysiological considerations. J. Chem. Neuroanat 2000;20:215–224. [PubMed: 11207420]

Hanakawa T, Fukuyama H, Katsumi Y, Honda M, Shibasaki H. Enhanced lateral premotor activity during paradoxical gait in Parkinson's disease. Ann. Neurol 1999;45:329–336. [PubMed: 10072047]

Hardman CD, Henderson JM, Finkelstein DI, Horne MK, Paxinos G, Halliday GM. Comparison of the basal ganglia in rats, marmosets, macaques, baboons, and humans: volume and neuronal number for the output, internal relay, and striatal modulating nuclei. J. Comp. Neurol 2002;445:238–255. [PubMed: 11920704]

Harik SI, LaManna JC, Snyder S, Wetherbee JR, Rosenthal M. Abnormalities of cerebral oxidative metabolism in animal models of Parkinson disease. Neurology 1982;32:382–389. [PubMed: 6278364]

Hattori S, Naoi M, Nishino H. Striatal dopamine turnover during treadmill running in the rat: relation to the speed of running. Brain Res. Bull 1994;35:41–49. [PubMed: 7953756]

Hays, W. Statistics for the Social Sciences. 2nd. Holt, Rinehart & Winston; New York: 1973.

Heise CE, Mitrofanis J. Evidence for a glutamatergic projection from the zona incerta to the basal ganglia of rats. J. Comp. Neurol 2004;468:482–495. [PubMed: 14689481]

Henderson JM, Pell M, O'Sullivan DJ, McCusker EA, Fung VS, Hedges P, Halliday GM. Postmortem analysis of bilateral subthalamic electrode implants in Parkinson's disease. Mov. Disord 2002;17:133–137. [PubMed: 11835450]

Hermer-Vazquez L, Hermer-Vazquez R, Moxon KA, Kuo KH, Viau V, Zhan Y, Chapin JK. Distinct temporal activity patterns in the rat M1 and red nucleus during skilled versus unskilled limb movement. Behav. Brain Res 2004;150:93–107. [PubMed: 15033283]

Holschneider DP, Scremin OU. Effects of ovariectomy on cerebral flow of rats. Neuroendocrinology 1998;67:260–268. [PubMed: 9588695]

Holschneider DP, Maarek JM, Harimoto J, Yang J, Scremin OU. An implantable bolus infusion pump for use in freely moving, nontethered rats. Am. J. Physiol.: Heart Circ. Physiol 2002;283:H1713–H1719. [PubMed: 12234827]

Holschneider DP, Maarek JM, Yang J, Harimoto J, Scremin OU. Functional brain mapping in freely moving rats during treadmill walking. J. Cereb. Blood Flow Metab 2003;23:925–932. [PubMed: 12902836]

Ichitani Y, Okamura H, Nakahara D, Nagatsu I, Ibata Y. Biochemical and immunocytochemical changes induced by intrastriatal 6-hydroxydopamine injection in the rat nigrostriatal dopamine neuron system: evidence for cell death in the substantia nigra. Exp. Neurol 1994;130:269–278. [PubMed: 7867756]

Ingvar M, Lindvall O, Stenevi U. Apomorphine-induced changes in local cerebral blood flow in normal rats and after lesions of the dopaminergic nigrostriatal bundle. Brain Res 1983;262:259–265. [PubMed: 6404503]

Jahanshahi M, Jenkins IH, Brown RG, Marsden CD, Passingham RE, Brooks DJ. Self-initiated versus externally triggered movements. I. An investigation using measurement of regional cerebral blood flow with PET and movement-related potentials in normal and Parkinson's disease subjects. Brain 1995;118(Pt 4):913–933. [PubMed: 7655888]

Jasmin L, Gogas KR, Ahlgren SC, Levine JD, Basbaum AI. Walking evokes a distinctive pattern of Fos-like immunoreactivity in the caudal brainstem and spinal cord of the rat. Neuroscience 1994;58:275–286. [PubMed: 8152539]

Jenkins IH, Fernandez W, Playford ED, Lees AJ, Frackowiak RS, Passingham RE, Brooks DJ. Impaired activation of the supplementary motor area in Parkinson's disease is reversed when akinesia is treated with apomorphine. Ann. Neurol 1992;32:749–757. [PubMed: 1471865]

Jones SC, Korfali E, Marshall SA. Cerebral blood flow with the indicator fractionation of [14C] iodoantipyrine: effect of PaCO2 on cerebral venous appearance time. J. Cereb. Blood Flow Metab 1991;11:236–241. [PubMed: 1900067]

Keri S, Gulyas B. Four facets of a single brain: behaviour, cerebral blood flow/metabolism, neuronal activity and neurotransmitter dynamics. NeuroReport 2003;14:1097–1106. [PubMed: 12821790]

Kolb B, Sutherland RJ, Whishaw IQ. A comparison of the contributions of the frontal and parietal association cortex to spatial localization in rats. Behav. Neurosci 1983;97:13–27. [PubMed: 6838719]

Kotter R, Feizelmeier M. Species-dependence and relationship of morphological and electrophysiological properties in nigral compacta neurons. Prog. Neurobiol 1998;54:619–632. [PubMed: 9550193]

Lavoie S, Drew T. Discharge characteristics of neurons in the red nucleus during voluntary gait modifications: a comparison with the motor cortex. J. Neurophysiol 2002;88:1791–1814. [PubMed: 12364507]

Lee JS, Ahn SH, Lee DS, Oh SH, Kim CS, Jeong JM, Park KS, Chung JK, Lee MC. Voxel-based statistical analysis of cerebral glucose metabolism in the rat cortical deafness model by 3D reconstruction of brain from autoradiographic images. Eur. J. Nucl. Med. Mol. Imaging 2005;32:696–701. [PubMed: 15747156]

Lees AJ. When did Ray Kennedy's Parkinson's disease begin? Mov. Disord 1992;7:110–116. [PubMed: 1584235]

Lindvall O, Ingvar M, Stenevi U. Effects of methamphetamine on blood flow in the caudate-putamen after lesions of the nigrostriatal dopaminergic bundle in the rat. Brain Res 1981;211:211–216. [PubMed: 7225839]

Ma J, Brudzynski SM, Leung LW. A role of subicular and hippocampal afterdischarges in initiation of locomotor activity in rats. Brain Res 1998;793:112–118. [PubMed: 9630556]

Massopust LC, Hauge DH, Ferneding JC, Doubek WG, Taylor JJ. Projection systems and terminal localization of dorsal column afferents: an autoradiographic and horseradish peroxidase study in the rat. J. Comp. Neurol 1985;237:533–544. [PubMed: 2413085]

Medina L, Reiner A. Neurotransmitter organization and connectivity of the basal ganglia in vertebrates: implications for the evolution of basal ganglia. Brain Behav. Evol 1995;46:235–258. [PubMed: 8564466]

Meissner W, Ravenscroft P, Reese R, Harnack D, Morgenstern R, Kupsch A, Klitgaard H, Bioulac B, Gross CE, Bezard E, Boraud T. Increased slow oscillatory activity in substantia nigra pars reticulata triggers abnormal involuntary movements in the 6-OHDA-lesioned rat in the presence of excessive extracellular striatal dopamine. Neurobiol. Dis 2006;22:586–598. [PubMed: 16531050]

Metz GA, Piecharka DM, Kleim JA, Whishaw IQ. Preserved ipsilateral-to-lesion motor map organization in the unilateral 6-OHDA-treated rat model of Parkinson's disease. Brain Res 2004;1026:126–135. [PubMed: 15476704]

Moore WH, Holschneider DP, Givrad TK, Maarek J-MI. Transcutaneous RF-Powered implantable minipump driven by a class-E transmitter. IEEE Trans. Biomed. Eng 2006;53:1–3.

Morgan S, Huston JP. The interhemispheric projection from the substantia nigra to the caudate-putamen as depicted by the anterograde transport of [3H]leucine. Behav. Brain Res 1990;38:155–162. [PubMed: 2363835]

Mraovitch S, Calando Y, Onteniente B, Peschanski M, Seylaz J. Cerebrovascular and metabolic uncoupling in the caudate-putamen following unilateral lesion of the mesencephalic dopaminergic neurons in the rat. Neurosci. Lett 1993;157:140–144. [PubMed: 8233044]

Nguyen PT, Holschneider DP, Maarek JM, Yang J, Mandelkern MA. Statistical parametric mapping applied to an autoradiographic study of cerebral activation during treadmill walking in rats. NeuroImage 2004;23:252–259. [PubMed: 15325372]

Nicholson SL, Brotchie JM. 5-hydroxytryptamine (5-HT, serotonin) and Parkinson's disease— Opportunities for novel therapeutics to reduce the problems of levodopa therapy. Eur. J. Neurol 2002;9(Suppl 3):1–6. [PubMed: 12464115]

Obeso JA, Rodriguez-Oroz MC, Rodriguez M, Macias R, Alvarez L, Guridi J, Vitek J, DeLong MR. Pathophysiologic basis of surgery for Parkinson's disease. Neurology 2000;55:S7–S12. [PubMed: 11188978]

Obeso JA, Rodriguez-Oroz MC, Lanciego JL, Rodriguez Diaz M. How does Parkinson's disease begin? The role of compensatory mechanisms. Trends Neurosci 2004;27:125–127. [PubMed: 15036875]

Pan WX, McNaughton N. The supramammillary area: its organization, functions and relationship to the hippocampus. Prog. Neurobiol 2004;74:127–166. [PubMed: 15556285]

Patlak CS, Blasberg RG, Fenstermacher JD. An evaluation of errors in the determination of blood flow by the indicator fractionation and tissue equilibration (Kety) methods. J. Cereb. Blood Flow Metab 1984;4:47–60. [PubMed: 6363433]

Paxinos, G.; Watson, C. The Rat Brain in Stereotactic Coordinates. 5th edition. Elsevier Academic Press; New York, NY.: 2005.

Pelled G, Bergman H, Goelman G. Bilateral overactivation of the sensorimotor cortex in the unilateral rodent model of Parkinson's disease—A functional magnetic resonance imaging study. Eur. J. Neurosci 2002;15:389–394. [PubMed: 11849305]

Perier C, Agid Y, Hirsch EC, Feger J. Ipsilateral and contralateral subthalamic activity after unilateral dopaminergic lesion. NeuroReport 2000a;11:3275–3278. [PubMed: 11043563]

Perier C, Vila M, Feger J, Agid Y, Hirsch EC. Functional activity of zona incerta neurons is altered after nigrostriatal denervation in hemiparkinsonian rats. Exp. Neurol 2000b;162:215–224. [PubMed: 10716902]

Playford ED, Jenkins IH, Passingham RE, Nutt J, Frackowiak RS, Brooks DJ. Impaired mesial frontal and putamen activation in Parkinson's disease: a positron emission tomography study. Ann. Neurol 1992;32:151–161. [PubMed: 1510355]

Rascol O, Sabatini U, Chollet F, Celsis P, Montastruc JL, Marc-Vergnes JP, Rascol A. Supplementary and primary sensory motor area activity in Parkinson's disease. Regional cerebral blood flow changes during finger movements and effects of apomorphine. Arch. Neurol 1992;49:144–148. [PubMed: 1736846]

Rascol O, Sabatini U, Chollet F, Fabre N, Senard JM, Montastruc JL, Celsis P, Marc-Vergnes JP, Rascol A. Normal activation of the supplementary motor area in patients with Parkinson's disease undergoing long-term treatment with levodopa. J. Neurol., Neurosurg. Psychiatry 1994;57:567–571. [PubMed: 8201325]

Rascol O, Sabatini U, Fabre N, Brefel C, Loubinoux I, Celsis P, Senard JM, Montastruc JL, Chollet F. The ipsilateral cerebellar hemisphere is overactive during hand movements in akinetic parkinsonian patients. Brain 1997;120(Pt 1):103–110. [PubMed: 9055801]

Rascol O, Sabatini U, Brefel C, Fabre N, Rai S, Senard JM, Celsis P, Viallard G, Montastruc JL, Chollet F. Cortical motor overactivation in parkinsonian patients with L-dopa-induced peak-dose dyskinesia. Brain 1998;121(Pt 3):527–533. [PubMed: 9549528]

Risold PY, Swanson LW. Chemoarchitecture of the rat lateral septal nucleus. Brain Res. Brain Res. Rev 1997;24:91–113. [PubMed: 9385453]

Roedter A, Winkler C, Samii M, Walter GF, Brandis A, Nikkhah G. Comparison of unilateral and bilateral intrastriatal 6-hydroxydopamine-induced axon terminal lesions: evidence for interhemispheric functional coupling of the two nigrostriatal pathways. J. Comp. Neurol 2001;432:217–229. [PubMed: 11241387]

Ruigrok, TJ. Precerebellar nuclei and red nucleus. In: Paxinos, G., editor. The Rat Nervous System. Elsevier Academic Press; San Diego: 2004. p. 167-204.

Ruigrok TJ, van der Burg H, Sabel-Goedknegt E. Locomotion coincides with c-Fos expression in related areas of inferior olive and cerebellar nuclei in the rat. Neurosci. Lett 1996;214:119–122. [PubMed: 8878098]

Sabatini U, Boulanouar K, Fabre N, Martin F, Carel C, Colonnese C, Bozzao L, Berry I, Montastruc JL, Chollet F, Rascol O. Cortical motor reorganization in akinetic patients with Parkinson's disease: a functional MRI study. Brain 2000;123(Pt 2):394–403. [PubMed: 10648446]

Sabol KE, Richards JB, Freed CR. In vivo dialysis measurements of dopamine and DOPAC in rats trained to turn on a circular treadmill. Pharmacol. Biochem. Behav 1990;36:21–28. [PubMed: 2349264]

Saint-Cyr JA, Woodward DJ. A topographic analysis of limbic and somatic inputs to the cerebellar cortex in the rat. Exp. Brain Res 1980;40:13–22. [PubMed: 7418756]

Sakurada O, Kennedy C, Jehle J, Brown JD, Carbin GL, Sokoloff L. Measurement of local cerebral blood flow with iodo [14C] antipyrine. Am. J. Physiol 1978;234:H59–H66. [PubMed: 623275]

Samuel M, Ceballos-Baumann AO, Blin J, Uema T, Boecker H, Passingham RE, Brooks DJ. Evidence for lateral premotor and parietal overactivity in Parkinson's disease during sequential and bimanual movements. A PET study. Brain 1997;120(Pt 6):963–976. [PubMed: 9217681]

Santori EM, Der T, Collins RC. Functional metabolic mapping during forelimb movement in rat. II. Stimulation of forelimb muscles. J. Neurosci 1986;6:463–474. [PubMed: 3950706]

Sauer H, Oertel WH. Progressive degeneration of nigrostriatal dopamine neurons following intrastriatal terminal lesions with 6-hydroxydopamine: a combined retrograde tracing and immunocytochemical study in the rat. Neuroscience 1994;59:401–415. [PubMed: 7516500]

Schallert T, Leasure JL, Kolb B. Experience-associated structural events, subependymal cellular proliferative activity, and functional recovery after injury to the central nervous system. J. Cereb. Blood Flow Metab 2000a;20:1513–1528. [PubMed: 11083226]

Schallert T, Fleming SM, Leasure JL, Tillerson JL, Bland ST. CNS plasticity and assessment of forelimb sensorimotor outcome in unilateral rat models of stroke, cortical ablation, parkinsonism and spinal cord injury. Neuropharmacology 2000b;39:777–787. [PubMed: 10699444]

Schwarting RK, Huston JP. Unilateral 6-hydroxydopamine lesions of meso-striatal dopamine neurons and their physiological sequelae. Prog. Neurobiol 1996a;49:215–266. [PubMed: 8878304]

Schwarting RK, Huston JP. The unilateral 6-hydroxydopamine lesion model in behavioral brain research. Analysis of functional deficits, recovery and treatments. Prog. Neurobiol 1996b;50:275–331. [PubMed: 8971983]

Smeets WJ, Marin O, Gonzalez A. Evolution of the basal ganglia: new perspectives through a comparative approach. J. Anat 2000;196(Pt 4):501–517. [PubMed: 10923983]

Swanson LW. The projections of the ventral tegmental area and adjacent regions: a combined fluorescent retrograde tracer and immunofluorescence study in the rat. Brain Res. Bull 1982;9:321–353. [PubMed: 6816390]

Taepavarapruk P, Floresco SB, Phillips AG. Hyperlocomotion and increased dopamine efflux in the rat nucleus accumbens evoked by electrical stimulation of the ventral subiculum: role of ionotropic glutamate and dopamine D1 receptors. Psychopharmacology (Berlin) 2000;151:242–251. [PubMed: 10972471]

Taghzouti K, Simon H, Tazi A, Dantzer R, Le Moal M. The effect of 6-OHDA lesions of the lateral septum on schedule-induced polydipsia. Behav. Brain Res 1985;15:1–8. [PubMed: 3919740]

Thevenaz P, Ruttimann UE, Unser M. A pyramid approach to subpixel registration based on intensity. IEEE Trans. Image Process 1998;7:27–41. [PubMed: 18267377]

Thobois S, Dominey P, Decety J, Pollak P, Gregoire MC, Broussolle E. Overactivation of primary motor cortex is asymmetrical in hemiparkinsonian patients. NeuroReport 2000;11:785–789. [PubMed: 10757520]

Van Uitert RL, Levy DE. Regional brain blood flow in the conscious gerbil. Stroke 1978;9:67–72. [PubMed: 341424]

Voges J, Volkmann J, Allert N, Lehrke R, Koulousakis A, Freund HJ, Sturm V. Bilateral high-frequency stimulation in the subthalamic nucleus for the treatment of Parkinson disease: correlation of therapeutic effect with anatomical electrode position. J. Neurosurg 2002;96:269–279. [PubMed: 11838801]

Waite JJ, Holschneider DP, Scremin OU. Selective immunotoxin-induced cholinergic deafferentation alters blood flow distribution in the cerebral cortex. Brain Res 1999;818:1–11. [PubMed: 9914432]

Yuan H, Sarre S, Ebinger G, Michotte Y. Histological, behavioural and neurochemical evaluation of medial forebrain bundle and striatal 6-OHDA lesions as rat models of Parkinson's disease. J. Neurosci. Methods 2005;144:35–45. [PubMed: 15848237]
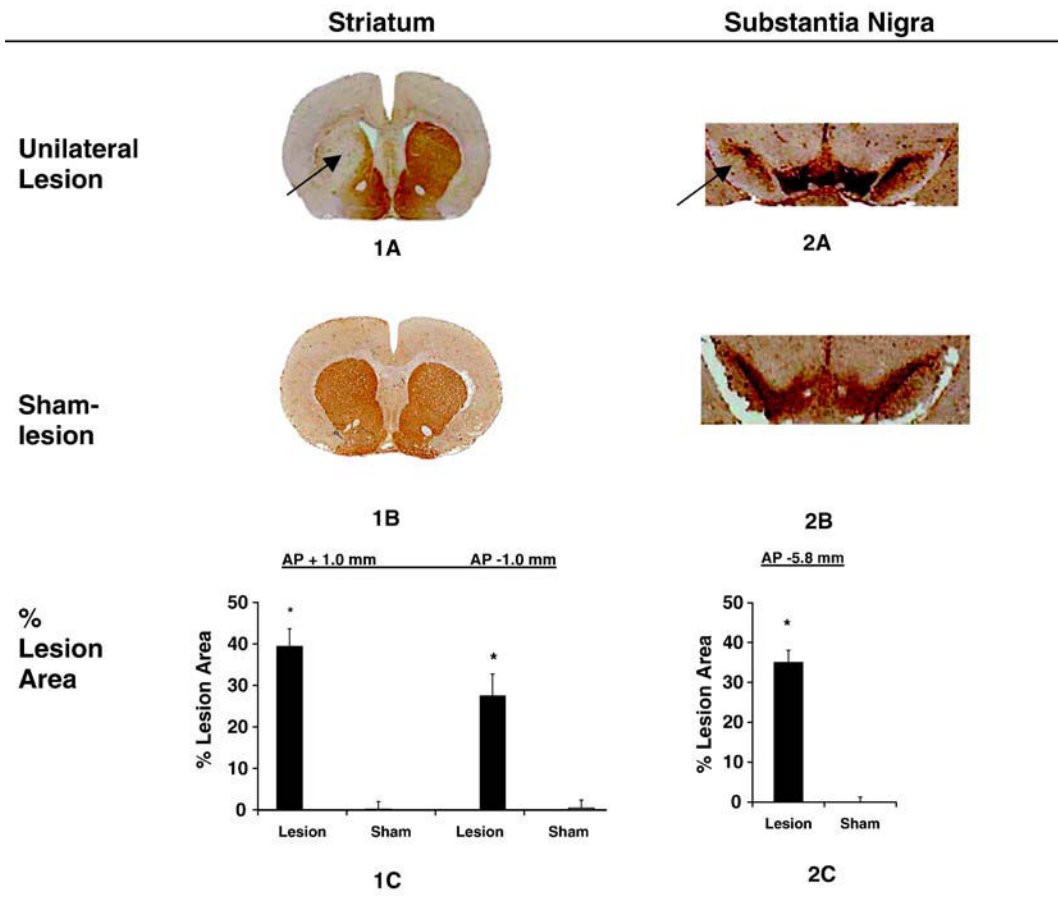
Fig. 1.
Lesion development in the striatum and substantia nigra. Coronal brain sections 33 days after unilateral intrastriatal injection of 6-OHDA (*n* = 18) or vehicle (*n* = 15) processed with TH-immunohistochemical and hematoxylin staining. The loss of area of TH-positive staining (arrows) on the lesioned side was expressed as a percentage of the total intact area, as measured on the contralateral side, both for the striatum (1C) and substantia nigra (2C). No detectable loss of TH staining was noted in sham-lesioned rats both at the level of the striatum and substantia nigra. Measurements (±S.E.M.) were taken at +1.0 mm and -1.0 mm relative to bregma (striatum) and -5.8 mm relative to bregma (substantia nigra). *$p < 0.0001$ vs. control.
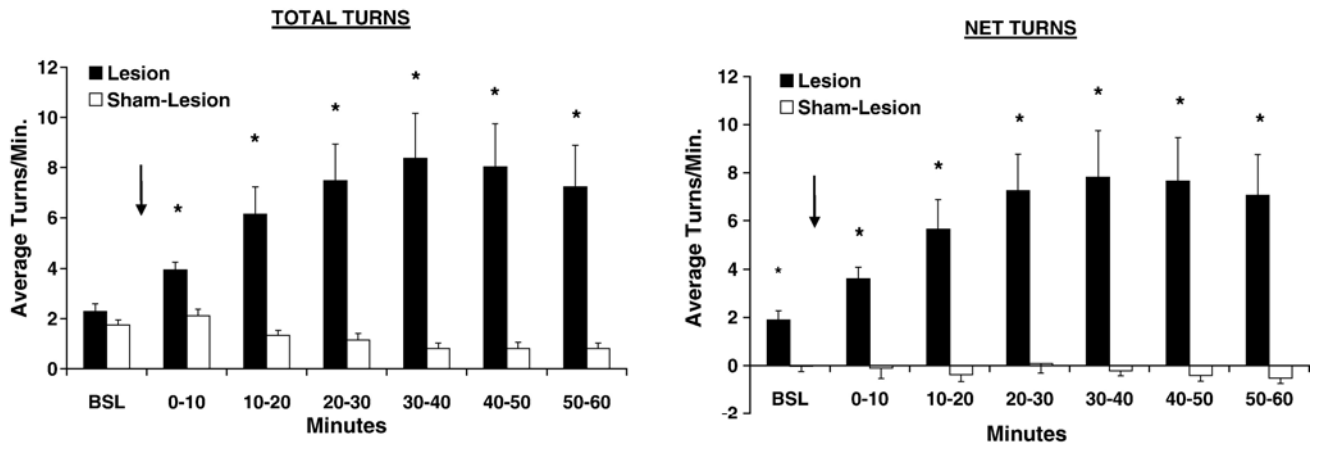
Fig. 2.
Rotational behavior (mean ± S.E.M.) after administration of D-amphetamine (5 mg/kg, i.p.) in rats with unilateral striatal lesions ($n = 18$) or sham lesions ($n = 15$). The left figure depicts total rotation; the right figure depicts net rotation (difference between positive clockwise turns and negative counter-clockwise turns). Injection occurs after a 10-min baseline, as indicated by the arrow. *$p < 0.005$ lesion vs. sham-lesion group.
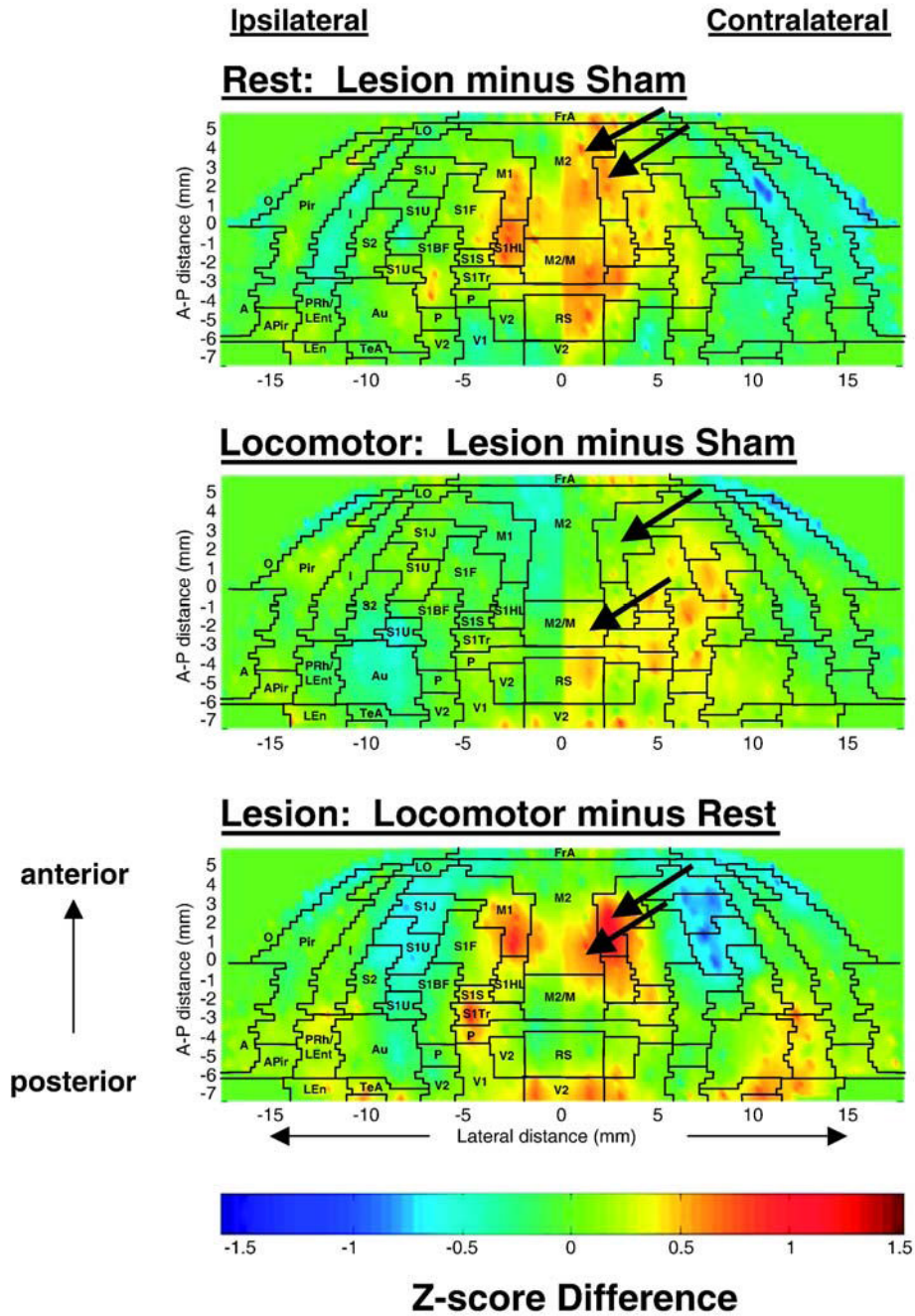
Fig. 3.
Maps of the color-coded average *z*-scores of regional cerebral blood flow related tissue radioactivity (CBF-TR) on the topographic surface of the flattened cortex. Depicted are average *z*-score differences between rats with unilateral striatal lesions and sham-lesioned animals either (top) at rest, or (middle) during treadmill walking. The comparison of the functional brain activation in response to treadmill walking is shown for the lesioned animals (bottom). Arrows denote changes in cerebral perfusion of motor cortex. In these two-dimensional maps of the flattened cortex, the *x*- and *y*-coordinates are obtained from measures of the anatomical distances within the autoradiographs. The *x*-axis (locations) represents lateral distance from the midline (in mm) along the cortical rim within a slice. The *y*-axis (slices) represents coronal

slices, numbered from rostral to caudal, with distance relative to bregma in millimeters (positive values being rostral to this landmark). To avoid discontinuities in the graphic representation, the space between each coronal slice and the locations within each slice, for which there were no measurements, was filled with values calculated by linear interpolation. Interpolations were performed separately for each hemisphere with interpolation distances ranging from 300 to 1000 μm. Superimposed on the maps are the borders of the main cortical areas (Paxinos and Watson, 2005): A, amygdala; Au, auditory; FrA, frontal association; I, insular; LEnt, lateral entorhinal; LO, lateral orbital frontal; M1, primary motor; M2, secondary motor; O, olfactory; P, parietal; Pir, piriform; PRh, perirhinal; RS, retrosplenial; primary somatosensory mapping the S1BF, barrel fields; S1FL, forelimbs; S1HL, hindlimbs; S1J, jaw; S1S, shoulder; S1Tr, trunk; S1U, upper lip region; S2, secondary somatosensory; TeA, temporal association; V1, primary visual; V2, secondary visual.
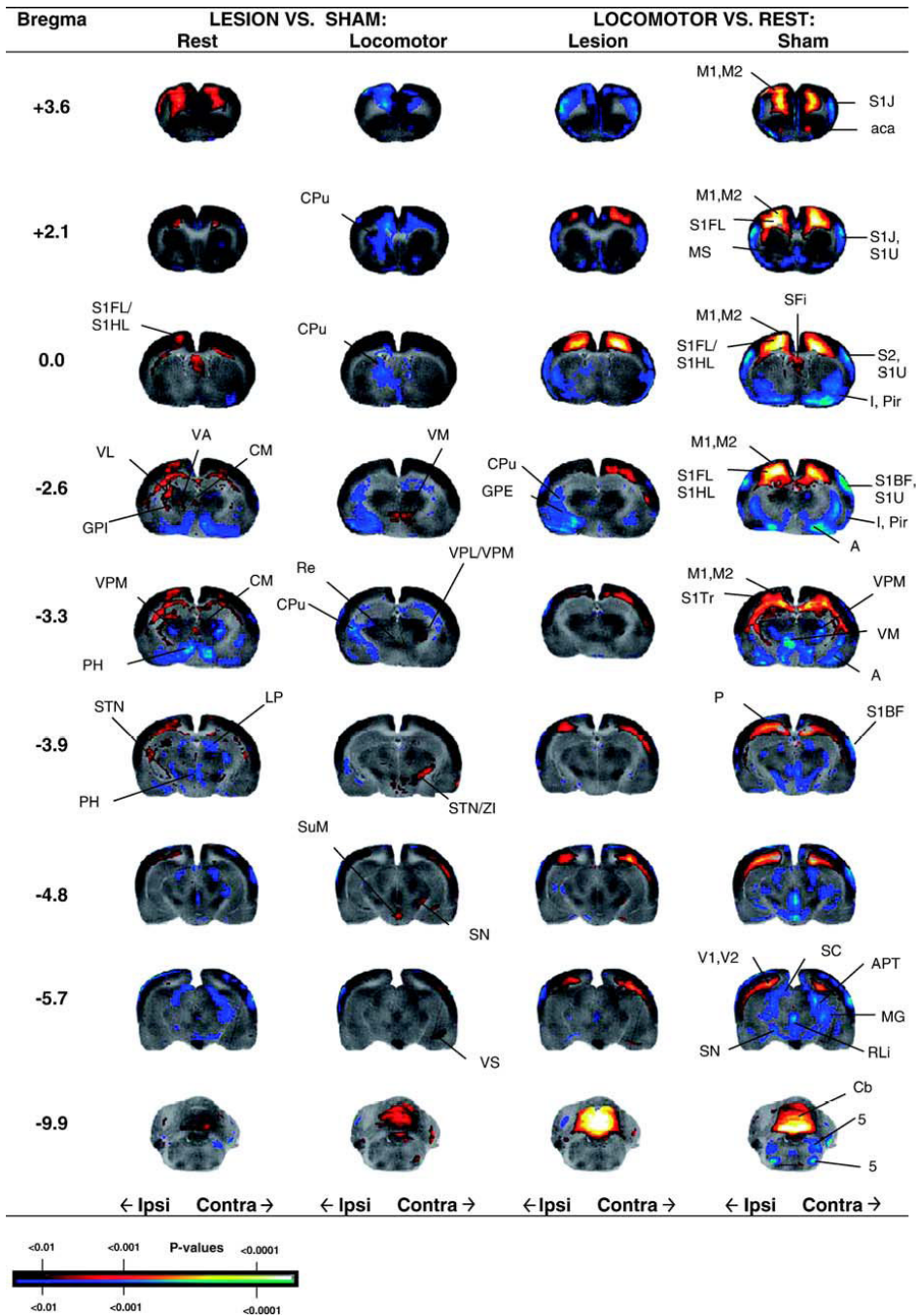
Fig. 4.

Regions of statistically significant differences of functional brain activation in rats with unilateral striatal lesions in lesioned and sham-lesioned rats either at rest (Lesion + Rest, $n =$ 9, Sham+ Rest, $n = 7$) or during a treadmill walking (Lesion+ Locomotor, $n = 9$, Sham+ Locomotor, $n = 8$). Depicted is a selection of representative coronal slices (anterior-posterior coordinates relative to bregma). Colored overlays show statistically significant positive (red) and negative (blue) differences (voxel level, $p < 0.01$). Abbreviations are those from the Paxinos and Watson (2002) rat atlas: 5 (trigeminal nucleus, motor, sensory), A (amygdala), aca (anterior commissures), APT (anterior pretectal nucleus), Cb (cerebellum), CM (central medial thalamic nucleus), CPu (striatum), GPE (external globus pallidus), GPI (internal globus pallidus), I

(insular cortex), LP (lateral posterior thalamic nucleus), M1, M2 (primary, secondary motor cortex), MG (medial geniculus), P (parietal cortex), S1BF, S1J, S1U, S1FL, S1HL, S1Tr (primary somatosensory cortex, barrel field, jaw, lip, forelimb, hindlimb, trunk), PH (posterior hypothalamus), Pir (piriform cortex), Re (thalamic reuinens nucleus), RLi (rostral linear raphe), SC (superior colliculus), SN (substantia nigra), STN (subthalamic nucleus), SuM (supramammillary nucleus), V1, V2 (primary and secondary visual cortex), VM (ventromedial thalamic nucleus), VL/VA (ventral lateral, ventral anterior thalamic nucleus), VPL/VPM (ventral posterolateral, ventral posteromedial thalamus), ZI (zona inserta).

Fig. 5.
Striato-pallidal circuits. Shown is the classic view of the indirect pathway (gray shading) and direct pathway (stipled box), as well as their net inhibitory (-) or excitatory (+) effects. STN (subthalamic nucleus), GPE (external globus pallidus), GPI/SNr (Internal globus pallidus/ substantia nigra reticulate), ventrolateral/ventral anterior thalamus (VL/VA). Adapted from DeLong and Wichmann (2007).
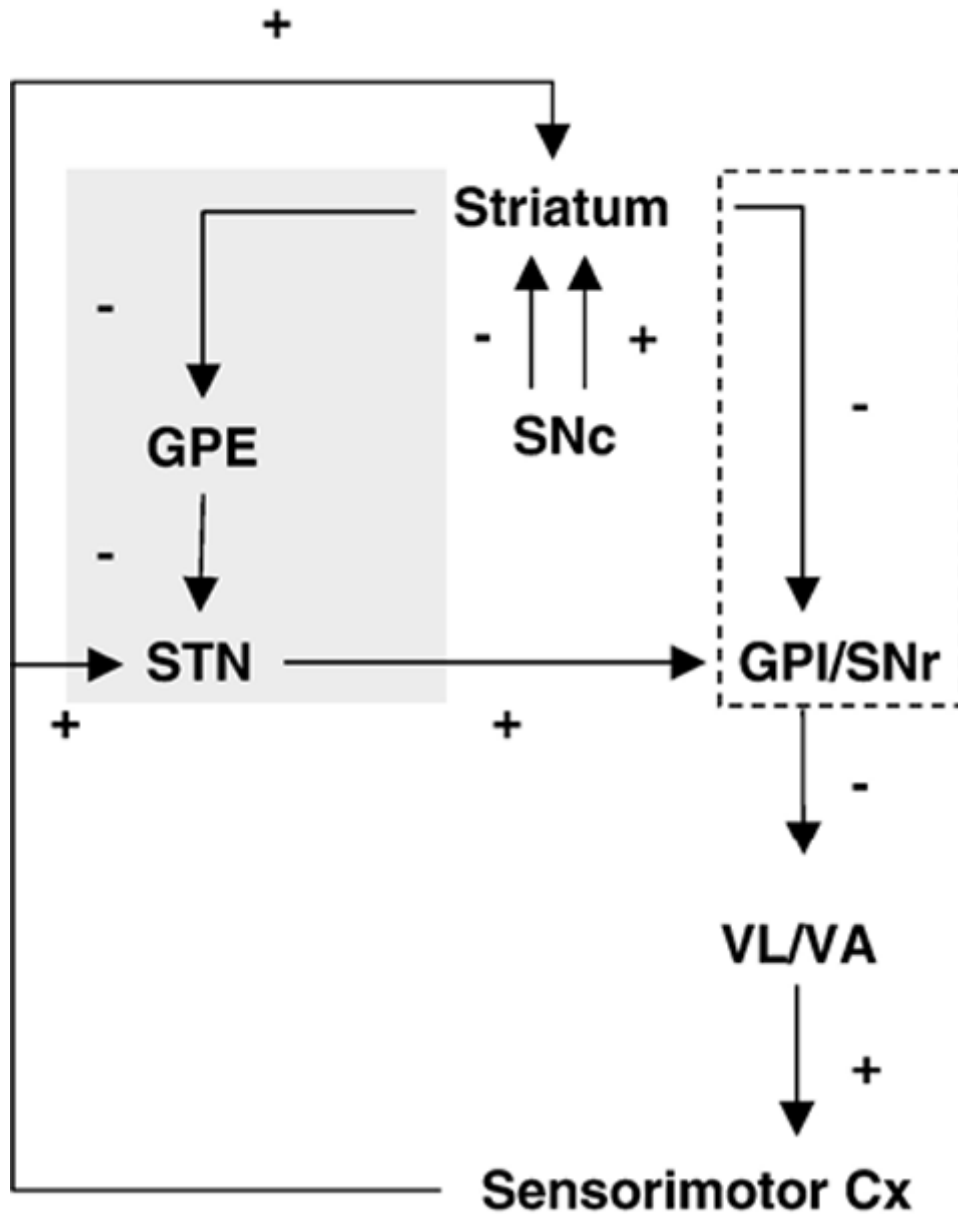
Table 1

Regions of statistically significant differences of functional brain activation on the surface of the flattened cortex as determined by ROI analysis

Bregma	Ipsilateral hemisphere										ROI #s					ROI #s							Contralateral hemisphere				
	10	9	8	7	6	5	4	3	2	1	1	2	3	4	5	6	7	8	9	10
A. Rest: Lesion vs. Sham																				
5.7	O	O	O	O	FrA	FrA	FrA	FrA	FrA	FrA	FrA	FrA	FrA	FrA	FrA	FrA	O	O	O	
5.4	O	O	O	O	FrA	FrA	FrA	FrA	FrA	FrA	FrA	FrA	FrA	FrA	FrA	FrA	O	O	O	
5.1	O	O	O	LO	LO	M2	M2	M2	M2	M2	M2	M2	M2	M2	M2	LO	O	O	O	
4.8	O	O	Pir	LO	LO	M1	M2	M2	M2	M2	M2	M2	M2	M1	M1	LO	LO	Pir	O	
4.5	O	Pir	LO	LO	M1	M1	M1	M1	M2	M2	M2	M2	M2	M1	M1	LO	LO	Pir	O	
4.2	O	Pir	LO		M1	M1	M1	M1	M2	M2	M2	M2	M2	M1	M1	LO		Pir	Pir	
3.9	O	Pir	LO		M1	M1	M1	M1	M2	M2	M2	M2	M1	M1	M1	M1		LO	Pir	
3.6	O	Pir	LO		S1J	S1J	M1	M1	M1	M2	M2	M1	M1	M1	M1	S1J		LO	Pir	
3.3	O	Pir	Pir		S1J	S1J	S1J	M1	M1	M2	M2	M1	M1	M1	S1J	S1J		LO	Pir	
3	O	Pir	Pir		S1J	S1J	S1J	M1	M1	M2	M2	M1	M1	S1J	S1J	S1J		Pir	Pir	
2.7	O	Pir	Pir		S1J	S1J	S1J	M1	M1	M2	M2	M1	M1	S1J	S1J	S1J		Pir	Pir	
2.4	O	Pir	Pir		S1J	S1J	S1FL	M1	M1	M2	M2	M1	M1	S1FL	S1J	S1J		Pir	Pir	
2.1	O	Pir	Pir		S1UL	S1J	S1FL	M1	M1	M2	M2	M1	M1	S1FL	S1J	S1UL		Pir	Pir	
1.8	O	Pir	Pir		S1UL	S1J	S1FL	S1FL	M1	M2	M2	M1	S1FL	S1FL	S1J	S1UL		Pir	Pir	
1.5	O	Pir	Pir		S1UL	S1J	S1FL	S1FL	M1	M2	M2	M1	S1FL	S1FL	S1J	S1UL		Pir	Pir	
1.2	O	Pir	Pir		S1UL	S1UL	S1FL	S1FL	M1	M2	M2	M1	S1FL	S1FL	S1UL	S1UL		Pir	Pir	
0.9	O	Pir	Pir		S1UL	S1UL	S1FL	S1FL	M1	M2	M2	M2	S1FL	S1FL	S1UL	S1UL		Pir	Pir	
0.6	O	Pir	Pir		S2	S1UL	S1FL	S1FL	M1	M2	M2	M2	S1FL	S1FL	S1UL	S2		Pir	Pir	
0.3	O	Pir	Pir		S2	S1UL	S1FL	S1FL	M1	M2	M2	M1	S1FL	S1FL	S1UL	S2		Pir	Pir	
0	O	Pir	Pir		S2	S1UL	S1FL	S1FL	M2	M2	M2	S1HL	S1FL	S1FL	S1UL	S2		Pir	A	O
−0.3		A	Pir		S2	S1UL	S1IBF	S1FL	S1HL	M2	M2	S1HL	S1FL	S1IBF	S1UL	S2		Pir	A	
−0.6		A	Pir		S2	S1UL	S1IBF	S1FL	S1HL	M2	M2	S1HL	S1FL	S1IBF	S1UL	S2		Pir	A	
−0.9		A	Pir		S2	S1BF	S1IBF	S1FL	S1HL	M2	M2	S1HL	S1FL	S1IBF	S1IBF	S2		Pir	A	
−1.2		A	Pir		S2	S1BF	S1IBF	S1FL	S1HL	M2/M1	M2/M1	S1HL	S1FL	S1IBF	S1BF	Au		Pir	A	
−1.5		A	Pir		S2	S1UL	S1IBF	S1Sh	S1HL	M2/M1	M2/M1	S1HL	S1Sh	S1IBF	S1UL	S2		Pir	A	
−1.8		A	Pir		S2	S1UL	S1IBF	S1Sh	S1HL	M2/M1	M2/M1	S1HL	S1Sh	S1IBF	S1UL	S2		Pir	A	
−2.1		A	Pir		S2	S1UL	S1IBF	S1Tr	S1HL	M2/M1	M2/M1	S1HL	S1Tr	S1IBF	S1UL	S2		Pir	A	
−2.4		A	Pir		S2	S1UL	S1BF	S1Tr	S1Tr	M2/M1	M2/M1	S1Tr	S1Tr	S1IBF	S1UL	S2		Pir	A	
−2.7		A	Pir		S2	S1UL	S1IBF	S1Tr	S1Tr	M2/M1	M2/M1	S1Tr	S1Tr	S1IBF	S1UL	S2		Pir	A	
−3		A	Pir	Pr/LEnt	Au	Au	S1IBF	P	P	P	P	P	S1Tr	S1IBF	S1UL	Au	Pr/LEnt	Pir	A	
−3.3		A	Pir	Pr/LEnt	Au	Au	S1IBF	P	P	P	P	P	S1Tr	S1IBF	S1UL	Au	Pr/LEnt	Pir	A	
−3.6		A	Pir	Pr/LEnt	Au	Au	S1BF	P	P	P	P	P	S1Tr	S1IBF	Au	Au	Pr/LEnt	Pir	A	
−3.9		A	Pir	Pr/LEnt	Au	Au	S1BF	P	P	P	P	P	P	S1IBF	Au	Au	Pr/LEnt	Pir	A	
−4.2		A	Pir	Pr/LEnt	Au	Au	P	V1	V2	RS	RS	V2	P	P	Au	Au	Pr/LEnt	Pir	A	
−4.5		A	APir	Pr/LEnt	Au	P	P	V1	V2	RS	RS	V2	V1	P	Au	Au	Pr/LEnt	APir	A	
−4.8		A	APir	Pr/LEnt	Au	P	P	V1	V2	RS	RS	V2	V1	P	Au	Au	Pr/LEnt	APir	A	
−5.1		A	APir	Pr/LEnt	Au	Au	P	V1	V2	RS	RS	V2	V1	P	Au	Au	Pr/LEnt	APir	A	
−5.4		A	APir	Pr/LEnt	Au	Au	V2	V1	V2	RS	RS	V2	V1	V2	Au	Au	Pr/LEnt	APir	A	
−5.7		A	APir	Pr/LEnt	Au	Au	V2	V1	V2	RS	RS	V2	V1	V2	Au	Au	Pr/LEnt	APir	A	
−6	APir	APir	APir	Pr/LEnt	Au	Au	V2	V1	V1	V2	V2	V1	V1	V2	Au	Au	Pr/LEnt	APir	APir	
−6.3			LEnt	LEnt	TeA	Au	V2	V1	V1	V2	V2	V1	V1	V2	Au	TeA	LEnt	LEnt		
−6.6			LEnt	LEnt	TeA	Au	V2	V1	V1	V2	V2	V1	V1	V2	Au	TeA	LEnt	LEnt		
−6.9			LEnt	LEnt	TeA	TeA	V2	V1	V1	V2	V2	V1	V1	V2	TeA	TeA	LEnt	LEnt		
−7.2			LEnt	LEnt	TeA	TeA	V2	V1	V1	V2	V2	V1	V1	V2	TeA	TeA	LEnt	LEnt		
−7.5			LEnt	LEnt	TeA	TeA	V2	V1	V1	V2	V2	V1	V1	V2	TeA	TeA	LEnt	LEnt		

B. Locomotor: Lesion vs. Sham

| 5.7 |
| 5.4 |
| 5.1 |
| 4.8 |
| 4.5 |
| 4.2 |
| 3.9 |
| 3.6 |
| 3.3 |
| 3 |
| 2.7 |
| 2.4 |
| 2.1 |
| 1.8 |
| 1.5 |
| 1.2 |
| 0.9 |
| 0.6 |
| 0.3 |
| 0 |
| −0.3 |
| −0.6 |
| −0.9 |
| −1.2 |
| −1.5 |
| −1.8 |
| −2.1 |
| −2.4 |
| −2.7 |
| −3 |
| −3.3 |
| −3.6 |
| −3.9 |
| −4.2 |
| −4.5 |
| −4.8 |
| −5.1 |
| −5.4 |
| −5.7 |
| −6 |
| −6.3 |
| −6.6 |
| −6.9 |
| −7.2 |
| −7.5 |

NIH-PA Author Manuscript

NIH-PA Author Manuscript

NIH-PA Author Manuscript

C. Lesion: Locomotor vs. Rest

D. Sham: Locomotor vs. Rest

Group comparisons are between *z*-scores of regional cortical perfusion. Shaded cells represent group differences significant at the *p* < 0.05 level. White text on a black background represents increases in cortical perfusion in each group comparison, i.e. *z*-score difference > 0. Black text on a gray background represent decreases in cortical perfusion for the comparison, i.e. *z*-score difference < 0. Rows represent coronal slices from rostral to caudal, with distances to bregma in millimeters. Within each slice cortical location nos. 1–10 are depicted from medial to lateral for both cerebral hemisphere (ipsilateral and contralateral to the striatal injections). Abbreviations of the anatomic regions are as defined in Fig. 3.

Table 2

Regions of statistically significant differences of functional brain activation as determined by SPM analysis

Region	Lesion vs. sham		Locomotor vs. rest	
	Rest (Ipsi/ Contra)	Locomotor (Ipsi/ Contra)	Lesion (Ipsi/ Contra)	Sham (Ipsi/ Contra)
Amygdala (BMA, BMP, MeA)	↓/↓ **	↓/- *	↓/↓ *	↓/↓ **
Anterior commissures (aca)	↑/-	↓/↓	↓/-	↑/↑ **
Cerebellum (vermis)	Midline ↑	Midline ↑ *	Midline ↑ *	Midline ↑ *
Corpus callosum (cc)	Midline ↑ *	Midline ↓	-	Midline ↑
Dentate gyrus (PoDG, posterior)	-/↓ *	-	↓/- *	↓/↓ **
External capsule (ec)	↑/↑ **	↓/↓ **	↑/↑	↑/↑ **
Forcepts minor (fmi)	↑/↑ **	↓/↓	-	↑/↑ **
Forcepts major (fmj)	↑/- *	-	↑/↑ **	↑/↑ **
Globus pallidus, external (GPE)	-	↓/- *	↓/- *	-
Globus pallidus, internal (GPI)	↑/- *	↓/- *	↓/-	-
Hypothalamus, anterior (AH), posterior (PH), posterior lateral (PLH)	↓/↓ **	-/↑	-	↓/↓ **
Inferior colliculus, central n. (CIC)	↓/↓ *	-	-	↓/↓ **
Lateral lemniscus (VLL, ILL)	↓/↓ *	-/↑	↓/↓ *	↓/↓
Medial septal n. (MS)	-	-	Midline ↓	Midline ↓ *
Pretectal n. anterior (APT)	↓/↓ *	-	↓/↓	↓/↓ **
Pretectal n., posterior (PPT)	-	-	-	↓/↓ **
Raphe, median (MnR)	Midline ↓	-	Midline ↓	Midline ↓ *
Red n. (RPC)	-	↑/↑	-	↓/↓ **
Septal n., lateral-medial, triangular, septofimbrial (LSI, TS, SFi)	Midline ↑ *	-	-	Midline ↑ *
Septal n., lateral ventral (LSV)	-	↓/-	↓/↓	-
Striatum, anterior dorsolateral (CPu)	-	↓/- *	-	↑/↑ **
Striatum, anterior centromedial (CPu)	↓/↓ **	↓/- *	-	-
Striatum, posterior ventral (CPu)	-/↓ *	↓/- *	↓/- *	↓/↓ **
Subiculum, posterior, dorsal, (Post, DS) Parasubiculum/Coudomedial Entorhinal Cx (PaS, CEnt)	-/↓ *	-/↑ *	-/↑ *	↓/↓ **
Subiculum, ventral (VS)	-	-/↑ *	-/↑	-
Substantia nigra, anterior (SN)	-	-/↑ *	-/↑	↓/↓ **
Subthalamic n. (STN)	↑/↑ *	-/↑ *	-/↑	↓/↓ **
Superior colliculus (SC)	↓/↓ *	↑/-	-	↓/↓
Supramammillary n. (SuM)	-	Midline ↑ *	-	Midline ↓ *
Thalamus, central, medial (CM)	Midline ↑	-	Midline ↓	Midline ↓ *
geniculate (medial, MG)	↓/↓ *	-	↓/- *	↓/↓ **
lateral dorsal (LD)	↑/- *	-	-	↑/↑ **
Lateral posterior (LP)	↓/↓ *	-	-	↓/↓ **
Reuinens n. (Re)	Midline ↓	Midline ↑		Midline ↓ *
Ventral lateral n. (VL)	↑/- *	-	-	-
Ventral anterior n. (VA)	↑/-	-	-	-
Ventroposterior lateral (VPL)	↑/- *	↑/↑	-	-
Ventroposterior medial (VPM)	↓/↓ *	-	↑/↑	↓/↓ **
Ventromedial, (VM)	↓/↓ **	↑/↑ **	-	↓/↓ **
Trigeminal n., motor, sensory, (5)	-	-/↑ *	↓/↑	↓/↓
Vestibular n., medial, superior (MVe, SuVe)	-	-/↑	-	↓/↓
Zona incerta	-	-/↑ *	-	↓/↓ **

Data are for rats with unilateral striatal lesions either at rest (Lesion + Rest, $n = 9$) or during a treadmill challenge (Lesion + Locomotor, $n = 9$), as well as for the corresponding sham-lesioned controls (Sham + Rest, $n = 7$; Sham + Locomotor, $n = 8$). Arrows denote increases or decreases in the group differences in cerebral blood flow tracer distribution (CBF-TR). Significance is for shown at the voxel level ($p < 0.01$).

*
designates additional significant at the cluster level with correction for multiple comparisons ($p < 0.01$, cluster $\geq$ 100 voxels).